

HYD 575

A. R. Schroeder HYD 575

BUREAU OF RECLAMATION
HYDRAULIC LABORATORY

UNITED STATES
DEPARTMENT OF THE INTERIOR
BUREAU OF RECLAMATION

**MASTER
FILE COPY**

DO NOT REMOVE FROM THIS FILE

ATTENUATION OF SURGE WAVES BY
A SIDE WEIR IN A TRAPEZOIDAL CHANNEL

Report No. Hyd-575

Hydraulics Branch
DIVISION OF RESEARCH



OFFICE OF CHIEF ENGINEER
DENVER, COLORADO

April 25, 1967

HYD 575

The information contained in this report may not be used in any publication, advertising, or other promotion in such a manner as to constitute an endorsement by the United States Government or the Bureau of Reclamation, either explicit or implicit, of any material, product, device, or process that may be referred to in the report.

Where approximate or nominal English units are used to express a value or range of values, the converted metric units in parentheses are also approximate or nominal. Where precise English units are used, the converted metric units are expressed as equally significant values.

CONTENTS

	<u>Page</u>
Abstract	iii
Acknowledgments	iv
Definition of Terms	v
Purpose	1
Conclusions	1
Theoretical Considerations	2
Development of a Simple Theoretical Relationship	2
Citrini's Equation for Attenuation of Surges in Rectangular Channels [4]	5
Limitations of Citrini's equation	6
The Experimental Investigation	6
Description of the Experimental Apparatus	6
Test Program and Limitations	8
Discussion of Experimental Results	8
Surge propagation in the channel without the side weir ...	8
Effect of the weir length on surge velocity	8
Effect of initial flow conditions on the surge attenua- tion efficiency of the side weir	9
Effects of the Froude number and the weir length on maximum and average surge heights at up- stream end of the weir	9
Agreement of theoretical predictions with the experimental results	10
Effect of using theoretical and experimental average surge velocities to solve the discharge balance equation	10
Effect of using different weir discharge coefficients to solve Citrini's equation	10
Effect of using different coefficients of mean effective head on the side weir	10
References	11
Appendix	31
	<u>Table</u>
Experimental Data for Initial Flow Depth of 0.333 Ft (10.15 cm)	1
Experimental Data for Initial Flow Depth of 0.320 Ft (9.75 cm)	2

CONTENTS--Continued

	<u>Figure</u>
Definition Sketch for Derivations	1
Typical Undular Form of Surge Wave	2
Experimental Test Channel	3
Control Device at Downstream End of Test Channel	4
Wave Probe Locations	5
Model Instrumentation	6
Bridge Circuit for Variable Capacitance Wave Probe	7
Variation of Average Surge Velocity with Froude Number of Initial Flow	8
Effect of Froude Number of Initial Flow on Attenuating Ability of Weir	9
Variation of Maximum Peaks and Average Surge Heights with Weir Length and Initial Flow Depth	10
Variation of the Two Theoretical Equations on Attenuation of Surge Waves	11
Variation of the Discharge Balance Equation with Different Average Surge Velocities	12
Variation of Citrini's Theory with the Weir Discharge Coefficient, 8.00-ft-long Weir, Initial Depth = 0.333 Ft	13
Variation of the Discharge Balance Equation with Different Coefficients of Mean Effective Head on the Side Weir	14

ABSTRACT

Theoretical equations and supporting experimental data are presented for determining attenuation of surge waves by a longitudinal side weir in a trapezoidal channel. Comparisons are made of a theoretical equation which had been derived previously for rectangular channels and an equation developed during this study; agreement of each of these equations with experimental data is determined. Surge heights were recorded by 6 capacitance-type wave probes with sensors consisting of plasticized-enamel-coated wire. Two short digital computer programs were developed for trial solutions of the theoretical equations. An explanation of each program, source statement listing, sample input data, and results are presented in the appendix.

DESCRIPTORS-- canals/ model tests/ *surges/ *trapezoidal channels/ weirs/ hydraulic transients// bore /wave// Froude number/ transitory waves/ unsteady flow/ calibrations/ instrumentation/ measuring instruments/ recording systems/ capacitance/ dielectrics/ electronic equipment/ research and development/ oscillographs/ computer programming/ mathematical analysis/ hydraulic models

IDENTIFIERS-- wave probes/ Citrini equation

ACKNOWLEDGMENTS

These studies were performed in the Hydraulics Branch, Division of Research of the Bureau of Reclamation. Photography was by W. M. Batts, Office Services Branch.

DEFINITION OF TERMS

A	Reciprocal of Froude number of initial flow
A_0	Cross sectional area of the channel with initial flow depth
C^*	Ratio of height of weir crest above channel floor to initial depth of flow
C_d	Weir discharge coefficient
D	Height of weir crest above channel floor
D_0	Hydraulic depth, $\frac{A_0}{T_0}$
D/S	Denotes downstream end of weir
dl	Derivative of the distance from upstream end of weir
F_0	Froude number of initial flow
g	Gravitational acceleration
h	Surge height above initial flow depth
h_{avg}	Average surge height
h_{max}	Maximum surge height
h_1	Average surge height at downstream end of weir (before attenuation)
h_2	Average surge height at upstream end of weir (after attenuation)
H_b	Depth of flow at side of main channel opposite weir (referenced to weir crest)
H_{eff}	Effective head on weir crest
H_m	Depth of flow along centerline of main channel (referenced to weir crest)
H_w	Depth of flow over side weir
K	Adjustment factor for shape of flow profile along side weir
L	Length of weir

Q or Q_{in}	Discharge entering upstream end of section
Q_o	Discharge over side weir
Q_{out}	Discharge of wave leaving upstream end of section (Q_w) plus discharge over side weir (Q_o)
Q_w	Discharge of wave after passing weir
T	Width of surge front at one-half of its height ($\frac{1}{2} h_2$) at upstream end of side weir
T_o	Top width of a trapezoidal channel at initial flow depth
U/S	Denotes upstream end of weir
V_o	Average velocity of initial flow
V_w	Average wave velocity
W	Width of channel at elevation of weir crest
Y	Average surge depth above channel floor ($Y_o + h_{avg}$)
Y_o	Depth of initial flow
y_f	Ratio of surge depth to initial depth at upstream end of weir
y_i	Ratio of surge depth to initial depth at downstream end of weir
μ	Dimensionless weir discharge coefficient = $C_d / \sqrt{2g}$

UNITED STATES
DEPARTMENT OF THE INTERIOR
BUREAU OF RECLAMATION

Office of Chief Engineer
Division of Research
Hydraulics Branch
Denver, Colorado
April 25, 1967

Report No. Hyd-575
Authors: S. Rungrongtaanin
D. L. King
Checked by: T. J. Rhone
Reviewed by: W. E. Wagner
Submitted by: H. M. Martin

ATTENUATION OF SURGE WAVES BY
A SIDE WEIR IN A TRAPEZOIDAL CHANNEL

PURPOSE

The purpose of this study was to determine the attenuating effect of longitudinal side weirs on surges initiated by rejection of canal flows. The study is an extension of previous work [9]^{1/} carried out in the Hydraulics Branch.

CONCLUSIONS

1. The surge wave velocity decreased as either the initial flow Froude number or the length of side weir increased.
2. The surge waves which were initiated from a high initial flow Froude number were attenuated more (in terms of percent reduction) than surges resulting from the flow at a low initial Froude number.
3. In determining the attenuation of surge waves by a side weir in a trapezoidal channel with the relative size and shape used in this study, and with Froude number less than 0.10, the studies showed that either maximum or average surge heights can be used in computations with no appreciable difference in results.
4. Citrini's equation, although originally developed for rectangular channels, was shown to be applicable to trapezoidal channels with the relative shape used in the present study and with small stable surges (h_{avg}/Y_0 less than 0.20).
5. There was no appreciable difference between the attenuations derived from the discharge balance equation using either a theoretical average surge velocity or an experimental average surge velocity.

^{1/}Numbers in brackets refer to references listed at the end of this report.

6. The use of different weir discharge coefficients in Citrini's equation provided only a slight change in the estimation of surge wave attenuation.

7. The theoretical curve derived from the discharge balance equation with a coefficient of mean effective head (K) on the side weir of about 1.75 showed the best agreement with the curve from Citrini's equation.

8. Citrini's equation predicted, within the limit of L/W less than 10, a surge height attenuation up to about 20 percent greater than that predicted by the discharge balance equation. Since considerable time is involved in solving Citrini's equation, the simpler discharge balance equation could be used for preliminary hand calculations.

THEORETICAL CONSIDERATIONS

Development of a Simple Theoretical Relationship

It is assumed that the initial depth of flow equals or nearly equals the height of the side weir crest above the channel floor, so that channel storage of the surge wave along the weir can be neglected. A definition sketch of a positive ascending (upstream) surge traveling along the weir is shown in Figure 1.

A simple balance of discharge following complete rejection gives:

$$Q_{in} = Q_{out}$$

where

Q_{in} = discharge entering upstream end of section (Q),
 Q_{out} = discharge of wave leaving upstream end of section (Q_w) +
discharge over weir (Q_o)

$$Q_{out} = Q_w + Q_o \quad (1)$$

$$Q_w = V_w T h_2$$

where

V_w = average wave velocity,
 T = width of surge front at one-half of its height ($\frac{1}{2} h_2$) at
upstream end of the side weir,
 h_2 = average surge height at upstream end of the side weir.

The theoretical average wave velocity (V_w) can be computed by trial and error from the equations

$$V_w = \sqrt{\frac{g(A_2 \bar{Y}_2 - A_1 \bar{Y}_1)}{A_1 \left(1 - \frac{A_1}{A_2}\right)}} - V_1$$

and

$$V_w = \frac{V_1 A_1 - V_2 A_2}{(A_1 - A_2)}$$

derived from the principles of continuity and momentum. \bar{Y}_1 and \bar{Y}_2 are centroidal depths. The subscripts refer to conditions before (1) and after (2) passage of the wave.

From the general weir equation, $Q_o = C_d L H^{1.5}$ the discharge over a side weir of length (L) is Q_o , and the head (H) is approximately ($Y-D$); therefore,

$$Q_o = C_d L (Y-D)^{1.5}$$

where

- Y = average surge depth above channel floor,
- C_d = weir discharge coefficient (with dimensions of $\sqrt{2g}$),
- L = Length of weir,
- D = height of weir crest above channel floor.

The flow over a side weir is spatially varied with decreasing discharge as described by Chow [3]. According to W. Frazer [6, p 314], the flow profile along the weir can be classified into five types. In the study described in this report, the flow profile might be considered as either Type 1 or 4, where Type 1 has critical depth at or near the entrance with supercritical flow in the weir section and the depth of flow decreasing along the weir; Type 4 has a depth of flow less than critical at the entrance with supercritical flow in the weir section and the depth of flow decreasing along the weir section. Flow in the main channel is subcritical in both cases.

From previous studies, [1], [2], [5] and [6], the accuracy of measurements of discharge capacity of side weirs mostly depends on the

mean effective head on the weir. Frazer [6] says, "Since the flow conditions at the weir are very complex, any treatment requires certain assumptions to be made. These assumptions are of such a nature that a detailed mathematical analysis is unjustified and inevitably experimental coefficients must be introduced. For this reason, the approach to the problem by several experimenters has been to obtain a simple formula, adjust the formula by experimental coefficients, and investigate the variation in the coefficients with the variation of the significant dimensionless variables obtained in the dimensional analysis."

In 1934, de Marchi, as discussed in V. K. Collinge's paper [5], published a theoretical equation to determine the discharge over a side weir in a rectangular channel. The equation was developed with the assumptions of constant total energy along the weir and conditions of steady flow. The equation is:

$$\frac{dQ_0}{d\ell} = C_d(Y - D)^{1.5}$$

From the results of Collinge's studies, he suggests that for small variations in depth the mean effective head on the weir should be taken as the mean value of $(Y - D)$ along the length of the weir. For large variations in depth the mean effective head should be calculated according to:

$$H_{\text{eff}} = \text{mean effective head} = \left\{ \frac{1}{L} \int_0^L (Y - D)^{1.5} d\ell \right\}^{2/3}$$

where

ℓ = distance along weir from upstream end of weir and L is the total length of the weir.

W. Frazer [6] suggests that the mean effective head on a side weir at any cross section of the channel, for the conditions of rapid flow in the weir section be determined by a variation of Simpson's rule:

$$H_{\text{eff}} = \frac{H_b + 4H_m + H_w}{6}$$

where

H_b = depth of flow at side of main channel opposite weir,
 H_m = depth of flow along centerline of main channel,
 H_w = depth of flow over side weir.

All depths are referenced to the crest of the weir.

In the present study, the flow conditions caused by surge waves along the side weir were extremely complicated, as clearly shown in Figure 2, so that conditions of steady flow did not exist. An accurate determination of the effective head could not be made without a rigorous analysis which was beyond the scope of this study.

Therefore, the approximate mean effective head on the side weir was estimated:

$$H_{\text{eff}} = \frac{h_1 + h_2}{2K}$$

where

- H_{eff} = mean effective head,
- h_1 = average surge height at downstream end of side weir,
- h_2 = average surge height at upstream end of side weir,
- K = factor of adjustment for nonlinear shape of flow profile along the weir.

Citrini's Equation for Attenuation of Surges in Rectangular Channels [4]

Citrini's equation was developed through the use of the method of characteristics. This is a more rigorous method of determining the action exerted by a longitudinal side weir on the height of positive waves, either ascending or descending, in a channel of rectangular section [4]. The validity of this equation has been checked by experiments [7] and [8]. The equation is:

$$y_f(y_f - 1) \left[1 + \frac{3}{4}(y_f - 1) \right] + (y_f^2 - y_i^2) \sqrt{\frac{1}{8}(y_f + y_i)} - y_i(y_i^2 - 1) \sqrt{\frac{1}{8}(y_f + 1)}$$

$$- \frac{\mu}{2} \frac{L}{W} A(y_f + y_i)^2 (y_f + y_i - 2C^*) \sqrt{\frac{1}{8}(y_f + y_i)(y_f + y_i - 2C^*)}$$

$$- \frac{y_f + y_i + A(y_f^2 - 1) \sqrt{\frac{1}{8}(y_f + 1)} + A(y_f - 1) \left[1 + \frac{3}{4}(y_f - 1) \right] + A(y_f + y_i) \sqrt{\frac{1}{2}(y_f + y_i)}}{2} = 0$$

in which

- y_i = ratio of surge depth to initial depth at downstream end of weir,
- y_f = ratio of surge depth to initial depth at upstream end of weir,
- μ = dimensionless weir discharge coefficient, $C_d/\sqrt{2g}$,
- L = weir length,

W = channel width,
A = reciprocal of Froude number of initial flow,
C* = ratio of height of weir crest above channel floor to initial depth of flow.

Solution of Citrini's equation is extremely complicated and subject to errors in calculation. A computer program, presented in the Appendix to this report, was prepared during an earlier study [9] to facilitate rapid calculation and to obtain a higher degree of reliability in the solution.

Limitations of Citrini's equation. --Citrini states that the accuracy of the equation deteriorates as L/W increases, with a maximum error of about 15 percent for L/W = 10. Also, the relationship was intended for use in determining the attenuation of the average surge height.

THE EXPERIMENTAL INVESTIGATION

Description of the Experimental Apparatus

The laboratory model used in these studies consisted of a portion of a model which had been developed for earlier studies [9]. The test channel had a depth of 1 foot (30.48 cm (centimeters)) and 1-1/2:1 side slopes, Figure 3. Most of the model was fabricated from plywood, with warped transition sections formed in concrete. The channel floor was level and the floor and sides had an enamel paint finish. Water was supplied through a recirculating system by a centrifugal pump. Discharge was measured with a portable orifice meter with interchangeable orifices, each of which was calibrated volumetrically. The test channel allowed weir lengths up to approximately 25 feet (7.6 m (meters)). Three weir lengths were tested; 8.00, 15.25 and 23.25 feet (2.44, 4.65, and 7.09 m). The weir crest was an ogee shape consisting of sheet metal formed over wood templates with elevation tolerances of plus or minus 0.002 feet (0.61 mm (millimeter)). The control at the downstream end of the model consisted of six slide gates which were used to control the depth of flow for each test discharge, Figure 4. The gates could be closed very rapidly for almost instantaneous and complete rejection of the inflow. Water surface elevations during each test run were measured with point gages at the centerline of the channel at the upstream and downstream ends of the weir.

The wave instrumentation is described in King's thesis [10]:

"The model instrumentation included six capacitance-type wave probes with sensors of plasticized-enamel-coated wire. Each wire was about 6-1/4 inches long (16 cm),

mounted in a U-shaped frame made from 1/4-inch-diameter (6.35 mm) stainless steel rod. The wires were held in the frames by small plastic insulators. The lower end of the wire was carefully sealed in the insulators to prevent electrical shorting by the water. Each frame was attached to a modified point gage staff in a rack and pinion device with a vernier reading to 0.001 foot (0.30 mm). Each probe was connected to one channel of a commercial six-channel direct-writing oscillograph."

The locations of the probes are shown on Figure 5. Figure 6 is a photograph of the test channel and model instrumentation.

"The wave height is indicated by the change in capacitance as the immersion of the sensor wire is changed. The plasticized enamel coating acts as the dielectric of the capacitor whose legs consist of the wire and the water. The unsealed end of the sensor wire is connected to one leg of a resistance-capacitance bridge, Figure 7. As the water level varies on the sensor, the capacitance across the fixed capacitor C_2 also varies, resulting in imbalance of the bridge and an accompanying signal to the recorder.

"Some difficulty was experienced in calibrating the probes and in maintaining this calibration over a reasonable period of time. Accurate data were assured by making a separate calibration for each test run, except in one or two cases when two runs at the same depth were made in quick succession. Calibration was accomplished by raising and lowering the probes known distances in a stable pool of water. Prewetting the wire by lowering the probe more than the required amount, waiting for several seconds, then raising the probe to the correct position, partially suppressed the nonlinearity caused by wetting. Fifteen to thirty minutes were required for the instrumentation to reach a stable condition. The probe was then raised in increments to the initial zero position to check the linearity. It was also necessary to carefully insulate the impedance-bridge circuit of each probe because of zero datum drift caused by room temperature variations.

"Other experimenters [12], by comparing wave probe records with photographic records, have estimated that meniscus (surface tension) effects can result in an error of approximately plus or minus 0.015 inch (0.4 mm) (or about 0.001 foot), with the largest errors occurring at wave troughs (-0.01 to +0.02 inch) (-0.25 mm to +0.5 mm). No attempt was made to

evaluate the surface tension effect in the present studies; however, the cited reference indicates that errors due to this effect are not appreciable."

Test Program and Limitations

Advanced planning is necessary to secure good results from model studies. Wasted time and inconvenience are avoided by making certain what type of information is required. Guided by the theoretical computations, test runs were planned so that for a given weir length rejected discharges between 0.131 and 0.397 cfs (cubic feet per second) (3.71 l/s and 11.24 l/s) could be investigated for two average flow depths in the channel: 0.333 foot (flow surface at the weir crest) and 0.320 foot (10.15 and 9.75 cm).

The experiments were concerned only with subcritical flow in the main channel. The values of the Froude number ($F_0 = V_0/\sqrt{gD_0}$, where $D_0 = A_0/T_0$) of the initial flow were between 0.061 and 0.200.

The maximum height of the first oscillation surge peak and the general characteristic shape of the wave profile were determined for each test. The studies were limited to the stable range (h_{avg}/Y_0 less than 0.20) [10], so that no breaking of the surge front would occur. The experimental data are shown on Tables 1 and 2.

Discussion of Experimental Results

Surge propagation in the channel without the side weir. --A series of tests [9] has been made with no side weir to determine the characteristics of the surge wave as it travels through the channel unattenuated by artificial means. The earlier observations apply equally to this study. The prototype rejection surge wave will be reduced by friction; however, in the length of channel under consideration for this study the maximum oscillation peak increased along the channel as the surge approached full development, followed by a fairly rapid decrease in size due to instability. The wave tended to become more stable as it traversed the channel. The general form of the rejection surge was undular, as described in the previous study [9].

Effect of the weir length on surge velocity. --Figure 8 shows the variation of average surge velocity through the channel reach with the Froude number of the initial flow. This diagram demonstrates the influence of the length of the side weir in reducing the velocity of the surge. Theoretically, the curves tend to converge to the value of the celerity of a gravity wave in still water at $F_0 = 0$. This convergence is seen in the data for the larger depth, but is not readily apparent in the data for the smaller depth over this particular range of Froude numbers. It can be concluded that the change in surge

velocity is due to two factors: (1) the higher initial flow velocity or Froude number causes retardation of the surge wave and (2) a greater weir length will discharge more water over the side weir and the resultant reduction of surge height will reduce the surge velocity.

Effect of initial flow conditions on the surge attenuation efficiency of the side weir. --Figure 9 shows that the efficiency of surge attenuation by a side weir directly depends on the initial flow conditions. The main factor affecting the surge attenuation is the discharge capacity of the side weir. The magnitude of this discharge is governed by the following initial flow factors: (1) The wave velocity controls the angle which the resultant velocity (vector sum of the wave velocity vector and the weir discharge velocity vector) makes with the side weir; in case of a high wave velocity (or low Froude number) the angle will be small and will provide less discharge capacity. This leads to a lower efficiency of surge attenuation. On the other hand, with low wave velocity (high F_0) the resultant velocity makes a greater angle with the weir and gives more discharge over the weir. (2) The mean effective head on the weir crest controls the magnitude of the discharge over the side weir. A relatively large mean effective head resulting from a surge initiated from a high Froude number will be attenuated more than one resulting from flow at a low Froude number.

Effects of the Froude number and the weir length on maximum and average surge heights at upstream end of the weir. --Figure 10 compares the experimental results for the relationships among Froude number, maximum and average surge heights at upstream end of the weir, and weir length. It should again be mentioned at this point that the recorded surge wave was of undular form, consisting of the initial wave followed by a series of secondary oscillations. In this study, the largest of the series usually was the leading peak. Consequently, the height of the first oscillation peak is considered as the maximum surge height throughout this report. The plots of the experimental data in Figure 10 show that in general, the maximum surge heights differ from the average surge heights only for Froude numbers greater than about 0.10. Based on these curves, it can be concluded that either the maximum or average surge height can be used in determining the amount of attenuation of surge waves by a side weir; assuming a trapezoidal channel with relative size and shape used in this study and a Froude number less than 0.10.

Figure 11 illustrates the experimental relationships between the weir length and the ratio of maximum and average surge depths at the upstream and downstream ends of the weir. The scatter in the data points is likely due to errors in determining the average surge heights from the oscillograph, especially at the upstream end of the weir where the wave form is unstable. Also included in the plot is a limiting asymptote which denotes no attenuation by the side weir.

Agreement of theoretical predictions with the experimental results. -- Figures 10 and 11 indicate that Citrini's equation, although originally developed for rectangular channels, is also applicable to trapezoidal channels with the same relative shape as that used in the present study and with relatively small stable surge waves (h_{avg}/Y_0 less than 0.20). The agreement between Citrini's theory and the experimental data is quite good. Through comparison of both theoretical curves, it appears that within a limit of $L/W = 10$ Citrini's equation shows a maximum deviation in surge height attenuation up to about 20 percent from that derived from the equation which was developed through the use of the discharge balance.

Effect of using theoretical and experimental average surge velocities to solve the discharge balance equation. -- Figure 12 shows that there is no appreciable difference between the attenuations predicted by the discharge balance equation using either the theoretical average surge velocity or experimental average surge velocity.

Effect of using different weir discharge coefficients to solve Citrini's equation. -- Figure 13 demonstrates that a difference in weir discharge coefficients causes only a slight change in the attenuation prediction. Therefore, for preliminary design purposes, the weir discharge coefficient can be considered as a relatively unimportant factor in surge wave attenuation evaluated by Citrini's equation.

Effect of using different coefficients of mean effective head on the side weir. -- Since the flow conditions caused by surge waves along a side weir are extremely complicated, no attempt was made to investigate the variables governing the mean effective head on the weir. However, the following approach was used to solve the problem in this study. According to Schoklitsch [13], the approximate mean effective head on a side weir is taken as the arithmetic mean of the heads at the upstream and downstream ends ($K = 1.0$), but this assumption is valid only in case of approximate linearity of the water surface profile. Consequently, in the case of nonlinearity such as occurred in this study where the undular profile exists along the weir section, it is necessary to modify the estimated mean head. A value of $K = 1.2$ was in the computations discussed thus far; 1.2 is the constant value of the ratio of maximum surge height to average surge height in a trapezoidal channel which was reported in previous studies [10]. Use of this value assumes that the average surge height is linear along the weir, but that the maximum surge height is curvilinear.

The value of K for deriving the discharge balance equation to provide the closest agreement with Citrini's equation can be determined from Figure 14. An initial flow depth of 0.333 foot (10.15 cm) and an 8.00-foot-long weir (2.44 m) were investigated. The results show that the required value of K is about 1.75. However, a K value of 1.0 is acceptable for initial estimates.

REFERENCES

1. Ackers, Peter, "A Theoretical Consideration of Side Weirs as Stormwater Overflows." Proceedings, Institution of Civil Engineers (England), Vol. 6, February 1957, p 250.
2. Allen, J. W., "The Discharge of Water Over Side Weirs in Circular Pipes." Proceedings, Institution of Civil Engineers (England), Vol. 6, February 1957, p 270.
3. Chow, V. T., "Rapidly Varied Unsteady Flow." Open Channel Hydraulics, Chapter 19, McGraw-Hill, 1959.
4. Citrini, Duilio, "Attenuation of a Positive Wave by Means of a Lateral Spillway, (Sull' attenuazione di un'onda positive ad opera di uno sfioratore)." Translated from the Italian by the U. S. Language Service Bureau, Translation No. 482, 1964.
5. Collinge, V. K., "The Discharge Capacity of Side Weirs." Proceedings, Institution of Civil Engineers (England), Vol. 6, February 1957, p 288.
6. Frazer, W., "The Behavior of Side Weirs in Prismatic Rectangular Channels." Proceedings, Institution of Civil Engineers (England), Vol. 6, February 1957, p 305.
7. Gentilini, Bruno, "The Action of a Side Weir on the Positive Wave Moving Upstream in an Open Channel, (L'Azione Di Uno Sfiatore Laterale Sull' onda Positive Ascendente in Un Canale)." Translated from the Italian by the U. S. Language Service Bureau, Translation No. 481, 1964.
8. De Marchi, Giulio, "Action of Side Weir and Tilting Gates on Translation Waves in Canals." Proceedings of the Minnesota International Hydraulics Conference, IAHR and ASCE, August 1953, p 537.
9. King, D. L., "Hydraulic Model Studies of Surges Developed by Rejection of Flow at the Forebay Pumping Plant, San Luis Unit-- Central Valley Project." Bureau of Reclamation, Hydraulic Laboratory Report No. Hyd-546, 1965.
10. King, D. L., "A Theoretical and Experimental Study of Rejection Surges in Trapezoidal Channels." Master's Thesis, University of Colorado, Boulder, Colorado, 1966.
11. Rayleigh, Lord, "On Waves." The London, Edinburgh, and Dublin Philosophical Magazine and Journal of Science, Ser. 5, Vol. 1, April 1876, pp 257-279.

12. Sandover, J. A., and Zienkiewicz, O. C., "Experiments on Surge Waves." Water Power, November 1957.
13. Schoklitsch, A., Hydraulic Structures, A Text and Handbook, translated from German by Samuel Shulits and reviewed by Lorenz G. Straub, published by the American Society of Mechanical Engineers, Vol. 1 (1937) pp 120-128.

Table 1

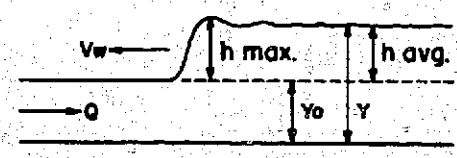
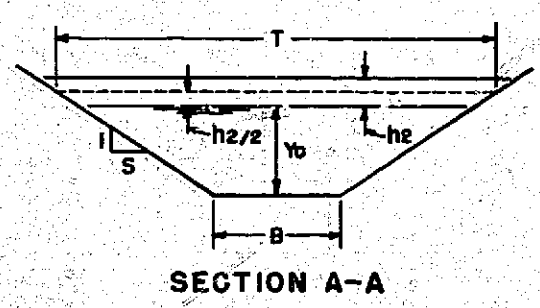
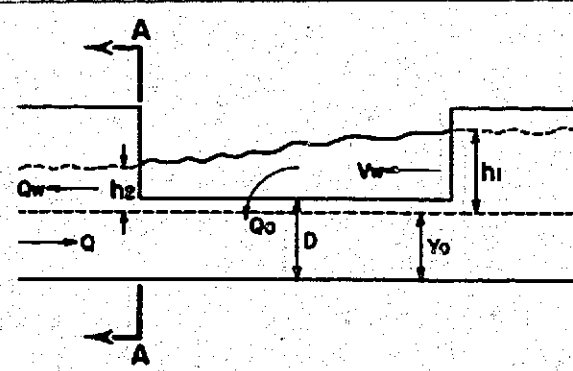
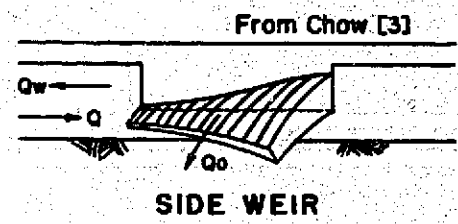
EXPERIMENTAL DATA FOR INITIAL FLOW DEPTH OF 0.333 FT (10.15 cm)

Side weir length L	Initial depth Y_0	F_0	Ave surge vel		Ratio of surge depth to Initial depth $(h+Y_0)/Y_0$				Percentage of first oscillation surge peak H_{max} recorded at: (end of weir)			
			ft/sec	(m/sec)	Average		First peak		D/S	1/3L	2/3L	U/S
					D/S	U/S	D/S	U/S				
8.00 ft (2.44 m)	0.333 ft (10.15 cm)	0.186 0.165 0.125 0.101 0.083 0.070 0.061	2.72 2.75 2.79 2.83 2.85 2.87 2.88	(0.83) (0.84) (0.85) (0.86) (0.87) (0.87) (0.88)	1.132	1.108	1.171	1.117	100	84.2	73.6	68.4
					1.120	1.096	1.150	1.102	100	82.0	72.0	68.0
					1.097	1.085	1.118	1.088	100	86.8	76.4	73.7
					1.079	1.064	1.088	1.066	100	82.8	82.8	75.9
					1.060	1.055	1.069	1.057	100	95.6	95.6	82.6
					1.054	1.045	1.060	1.045	100	90.0	75.0	75.0
					1.048	1.039	1.051	1.039	100	94.1	82.3	76.5
					1.057	1.042	1.057	1.042	100	85.7	69.4	55.1
15.25 ft (4.65 m)	0.333 ft (10.15 cm)	0.186 0.165 0.125 0.099 0.083 0.070 0.062	2.67 2.70 2.76 2.80 2.83 2.84 2.86	(0.81) (0.82) (0.84) (0.85) (0.86) (0.87) (0.87)	1.132	1.084	1.146	1.084	100	85.7	69.4	55.1
					1.120	1.080	1.143	1.080	100	75.0	66.7	56.2
					1.090	1.069	1.109	1.069	100	80.5	69.4	66.7
					1.072	1.053	1.080	1.053	100	85.2	70.4	66.7
					1.060	1.052	1.069	1.054	100	87.0	78.3	78.3
					1.058	1.044	1.059	1.044	100	85.0	80.0	75.0
					1.057	1.042	1.057	1.042	100	89.5	84.2	73.7
					1.057	1.042	1.057	1.042	100	85.7	69.4	55.1
23.25 ft (7.09 m)	0.333 ft (10.15 cm)	0.186 0.166 0.124 0.098 0.082 0.071 0.062	2.61 2.66 2.73 2.76 2.79 2.81 2.83	(0.80) (0.81) (0.83) (0.84) (0.85) (0.86) (0.86)	1.132	1.067	1.164	1.068	100	74.5	58.2	41.8
					1.132	1.066	1.148	1.066	100	81.6	79.6	44.9
					1.084	1.050	1.101	1.050	100	79.4	61.8	50.0
					1.065	1.039	1.075	1.039	100	80.0	68.0	52.0
					1.063	1.044	1.066	1.044	100	87.0	78.3	65.2
					1.057	1.044	1.062	1.044	100	85.7	85.7	71.4
					1.048	1.039	1.051	1.039	100	100.0	82.3	76.5
					1.048	1.039	1.051	1.039	100	100.0	82.3	76.5

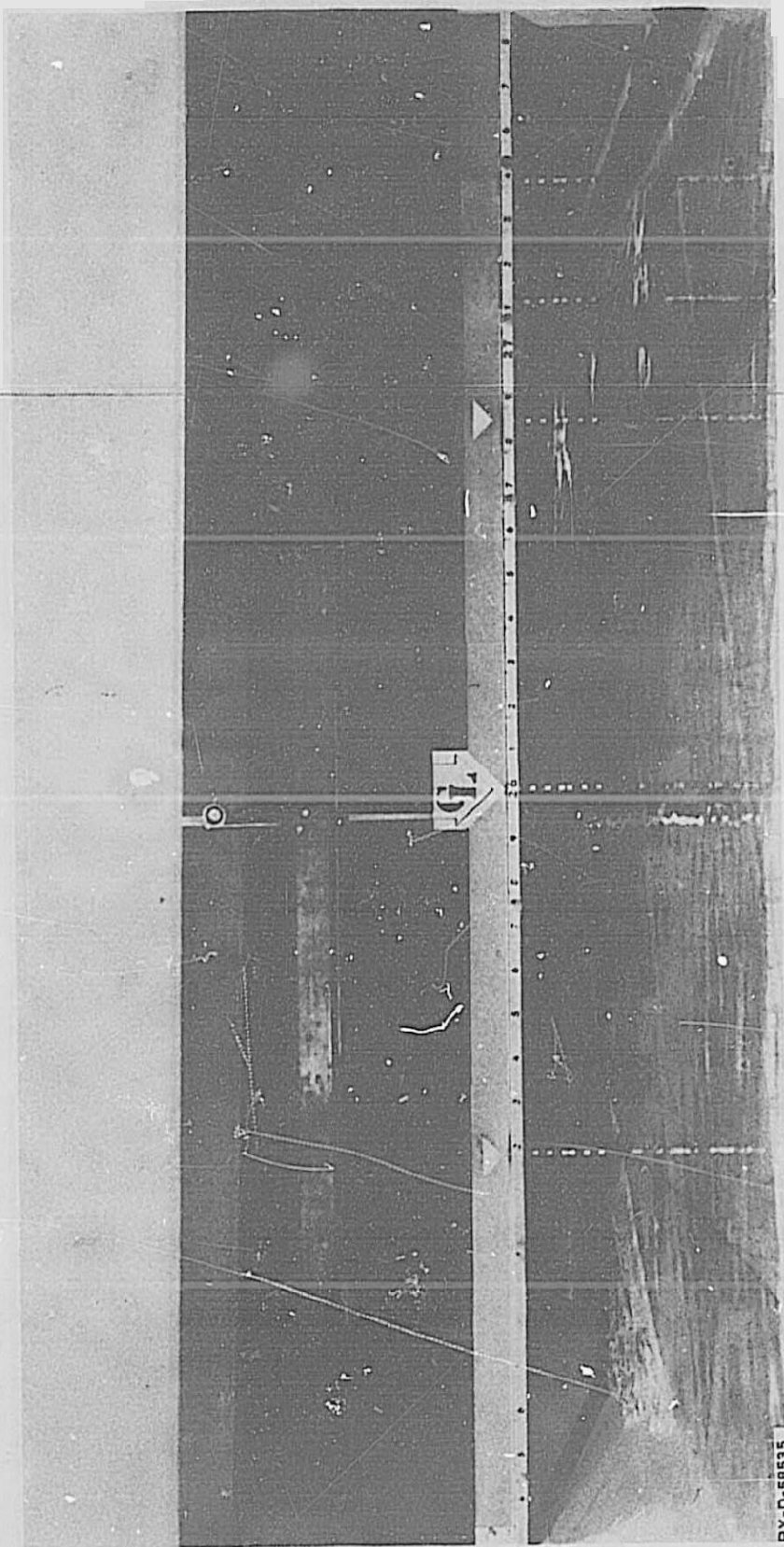
Table 2

EXPERIMENTAL DATA FOR INITIAL FLOW DEPTH OF 0.320 FT (9.75 cm)

Side weir length L	Initial depth Y_0	F _o	Ave surge vel		Ratio of surge depth to initial depth $(h+Y_0)/Y_0$			Percentage of first oscillation surge peak H_{max} recorded at: (end of weir)																															
			ft/sec	(m/sec)	Average		First peak	D/S																															
					D/S	U/S		D/S	U/S	1/3 L	2/3 L	U/S																											
8.00 ft (2.44 m)	0.320 ft (9.75 cm)	0.198	2.61	(0.80)	1.149	1.130	1.167	1.139	100	96.3	88.9	83.3	80.4																										
														0.177	2.63	(0.80)	1.137	1.119	1.159	1.128	100	86.3	84.3	89.7	83.3														
														0.133	2.66	(0.81)	1.113	1.100	1.122	1.109	100	92.3	92.3	86.7	87.5	90.0													
														0.105	2.74	(0.84)	1.084	1.078	1.093	1.078	100	86.7	86.7	91.7	94.7	94.7													
														0.087	2.75	(0.84)	1.069	1.062	1.075	1.065	100	100	100	95.0	95.0	94.7													
														0.074	2.77	(0.84)	1.061	1.055	1.061	1.055	100	100	100	95.0	95.0	94.7													
														0.065	2.79	(0.85)	1.059	1.053	1.059	1.055	100	100	100	94.7	94.7	94.7													
														15.25 ft (4.65 m)	0.320 ft (9.75 cm)	0.200	2.58	(0.79)	1.131	1.106	1.169	1.113	100	96.3	77.8	66.7	70.8												
																												0.177	2.62	(0.80)	1.125	1.100	1.150	1.106	100	85.4	79.2	74.3	82.7
																												0.132	2.64	(0.80)	1.093	1.084	1.109	1.084	100	91.4	77.1	86.2	91.7
0.105	2.69	(0.82)	1.081	1.075	1.091	1.075	100	89.6	86.2	91.7	95.0	94.7																											
0.087	2.72	(0.83)	1.068	1.065	1.075	1.065	100	100	100	95.0	95.0	94.7																											
0.075	2.74	(0.84)	1.062	1.059	1.062	1.059	100	100	100	95.0	95.0	94.7																											
0.065	2.76	(0.84)	1.059	1.056	1.059	1.056	100	100	100	94.7	94.7	94.7																											
23.25 ft (7.09 m)	0.320 ft (9.75 cm)	0.200	2.54	(0.77)	1.150	1.103	1.175	1.103	100	83.9	71.4	58.9	66.7																										
																												0.179	2.59	(0.79)	1.138	1.100	1.160	1.107	100	84.3	76.5	79.4	84.0
																												0.134	2.66	(0.81)	1.097	1.081	1.107	1.085	100	97.1	88.2	75.0	84.0
														0.107	2.68	(0.82)	1.081	1.053	1.088	1.053	100	85.7	75.0	92.0	100														
														0.086	2.70	(0.82)	1.067	1.058	1.077	1.065	100	92.0	92.0	100	100														
														0.076	2.71	(0.83)	1.066	1.063	1.069	1.069	100	100	100	100	100														
														0.065	2.73	(0.83)	1.052	1.049	1.059	1.059	100	100	100	100	100														



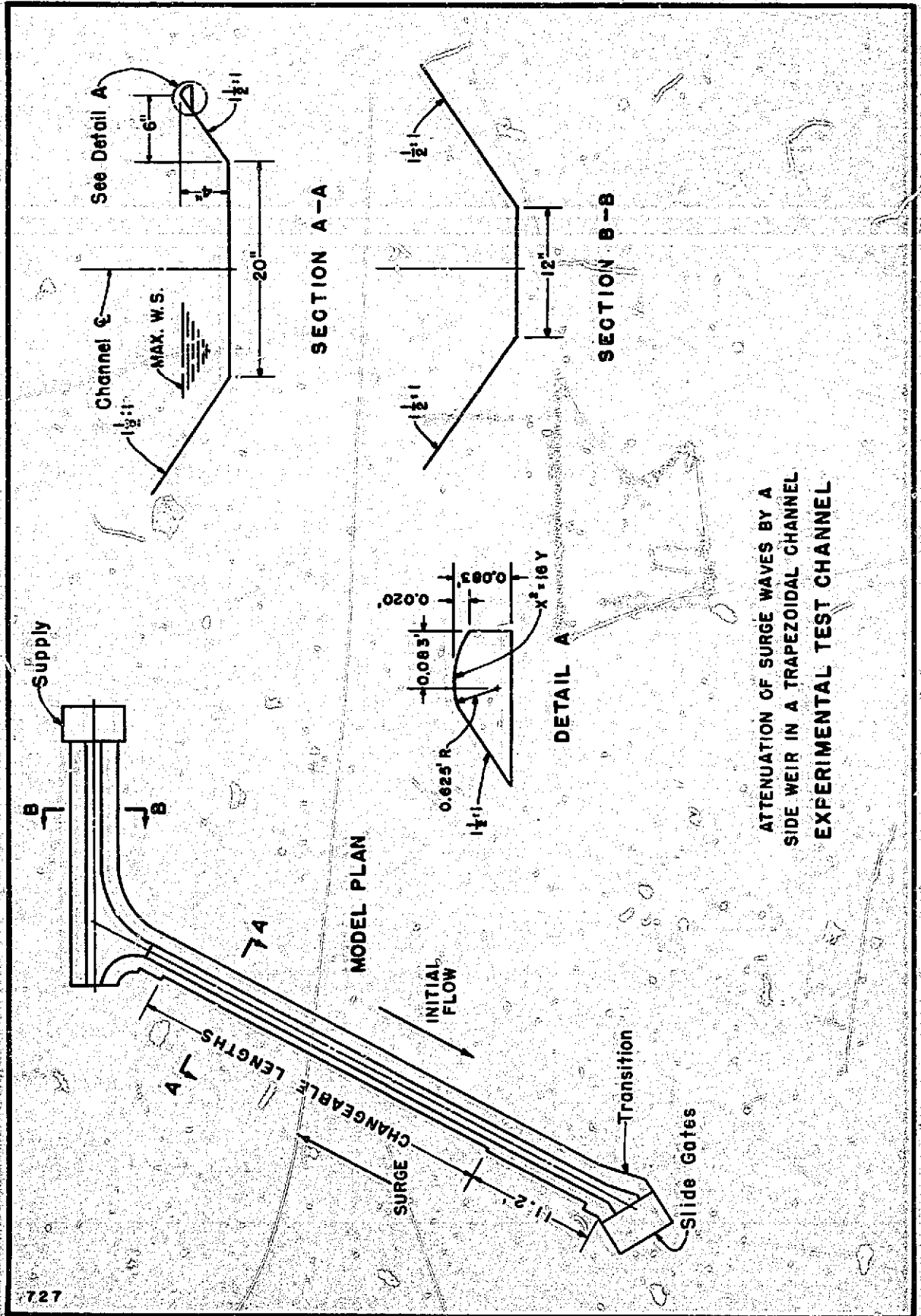
ATTENUATION OF SURGE WAVES BY A
SIDE WEIR IN A TRAPEZOIDAL CHANNEL
DEFINITION SKETCH FOR DERIVATIONS



PX-D-58535

ATTENUATION OF SURGE WAVES BY A
SIDE WEIR IN A TRAPEZOIDAL CHANNEL.

Typical Undular Form of Surge Wave
Along the Weir Crest Looking Downstream



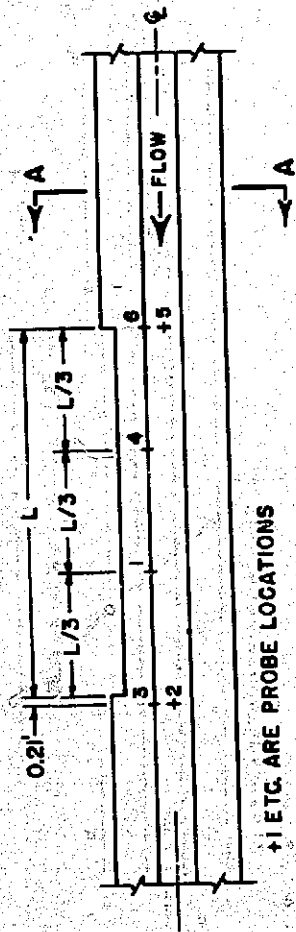
ATTENUATION OF SURGE WAVES BY A
SIDE WEIR IN A TRAPEZOIDAL CHANNEL
EXPERIMENTAL TEST CHANNEL



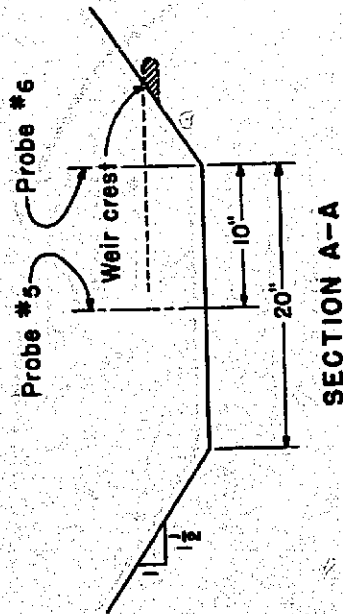
NOTE: Backflow tanks were not used in this study.

**ATTENUATION OF SURGE WAVES BY A
SIDE WEIR IN A TRAPEZOIDAL CHANNEL**

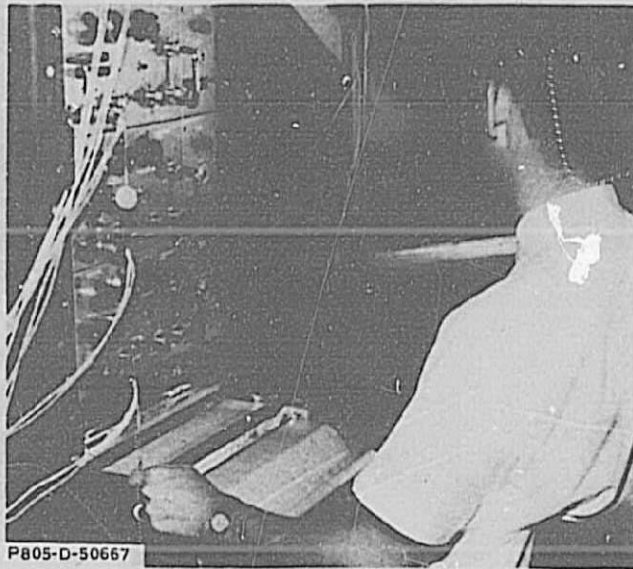
**Control Device at Downstream End
of Test Channel**



WEIR LENGTH L (FT.)	DISTANCE OF L/3 (FT.)
8.00	2.67
15.25	5.08
23.25	7.75



ATTENUATION OF SURGE WAVES BY A
SIDE WEIR IN A TRAPEZOIDAL CHANNEL
WAVE PROBE LOCATIONS



A. Wave probe and recorder



B. Capacitance wave probe

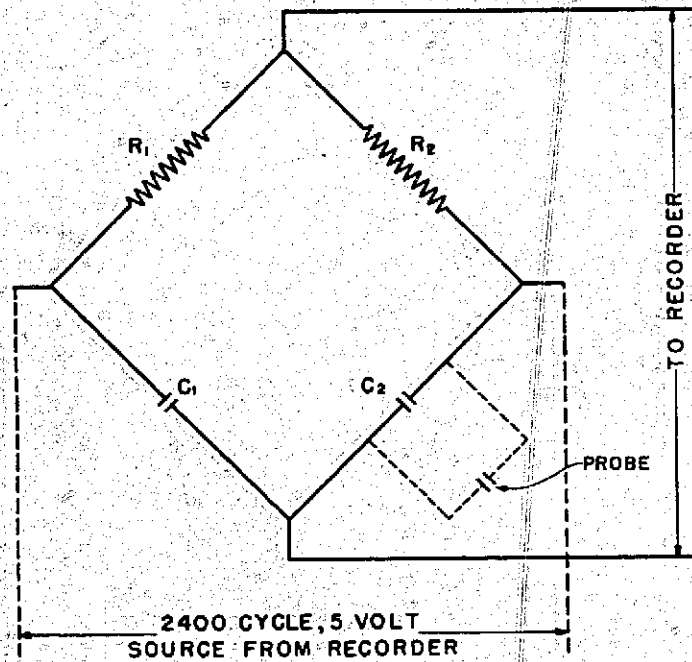


C. Passage of surge wave along weir

ATTENUATION OF SURGE WAVES BY A
SIDE WEIR IN A TRAPEZOIDAL CHANNEL

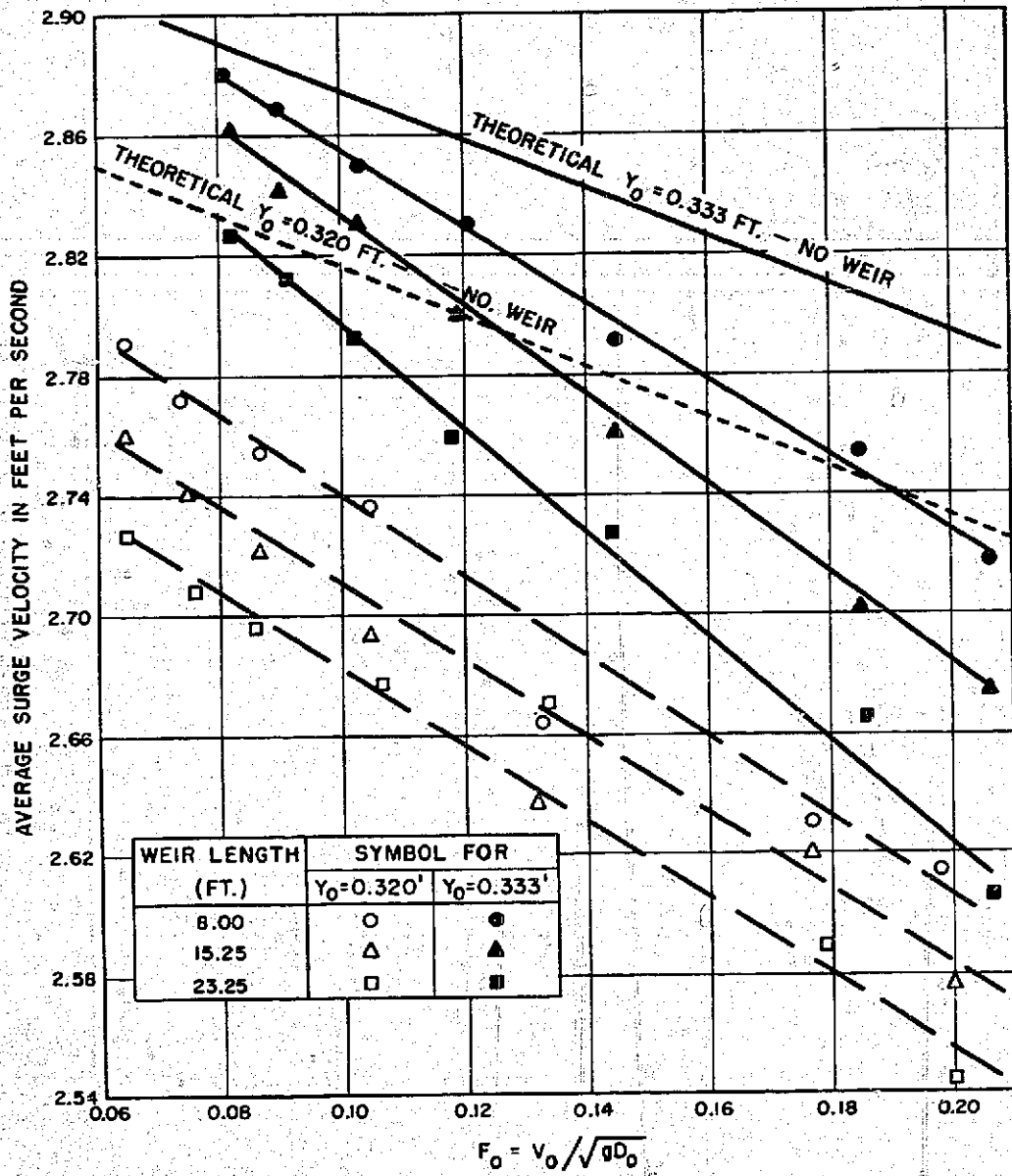
Model Instrumentation

$R_1, R_2 = 200$ to 250 ohms.
 $C_1, C_2 = 0.1$ microfarad, dual bathtub
condenser preferred.
From King [10]

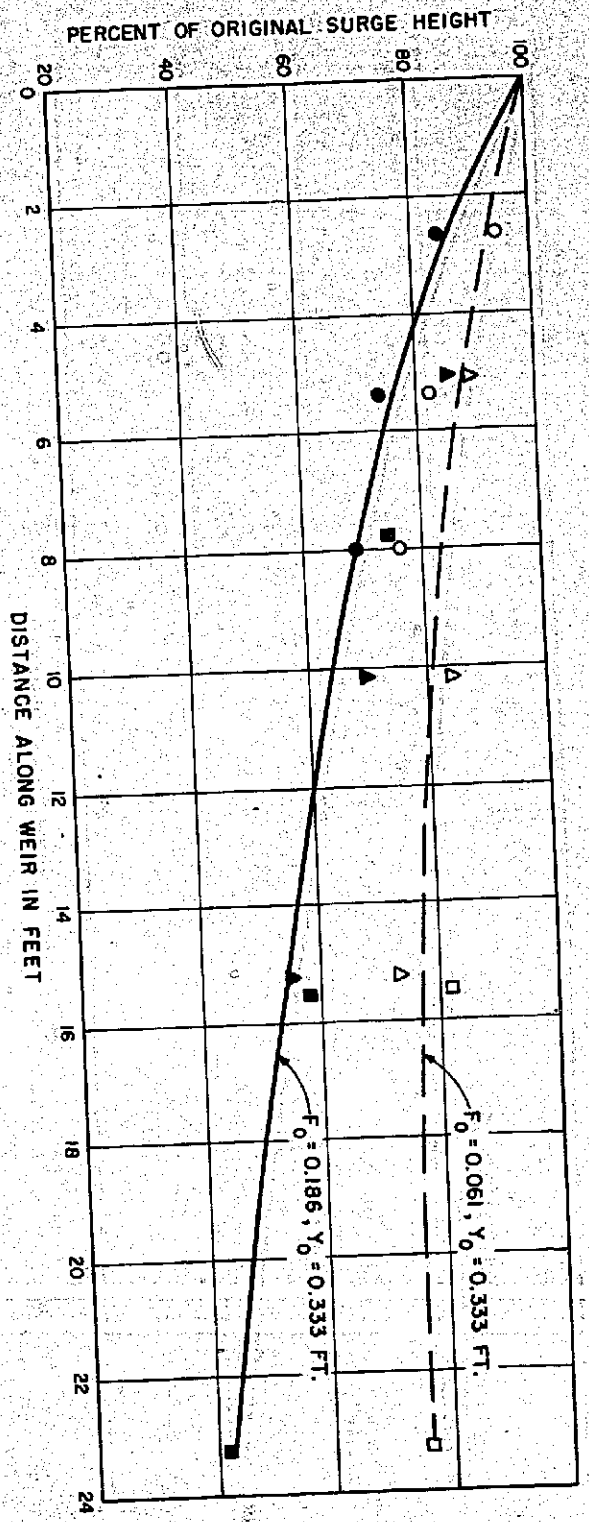


ATTENUATION OF SURGE WAVES BY A
SIDE WEIR IN A TRAPEZOIDAL CHANNEL
BRIDGE CIRCUIT FOR VARIABLE CAPACITANCE WAVE PROBE

Figure 8
Report Hyd-575



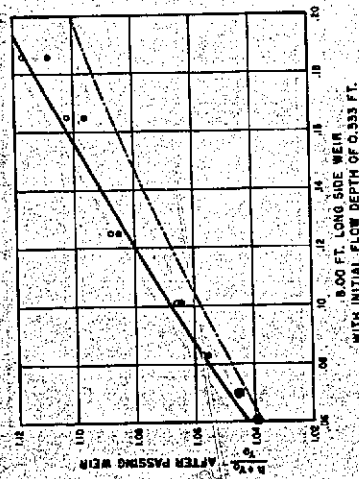
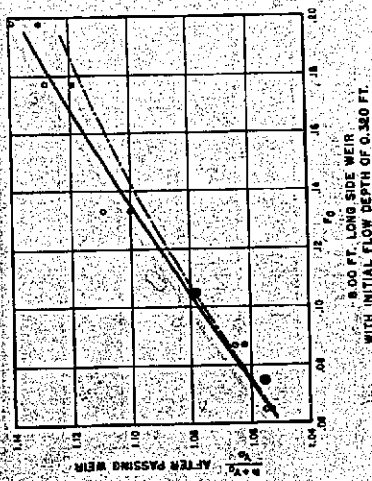
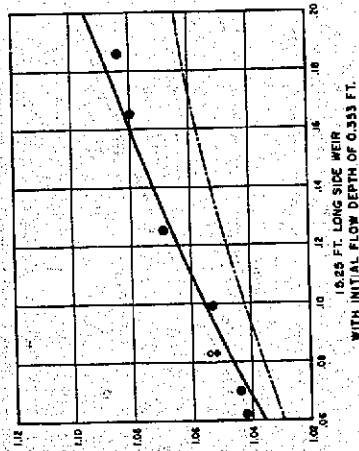
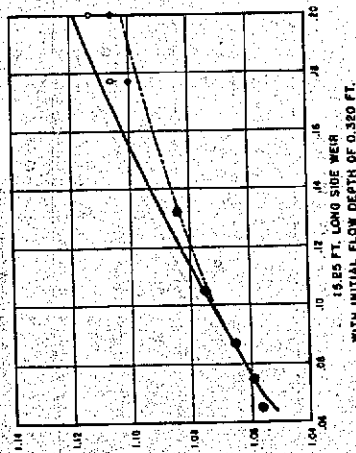
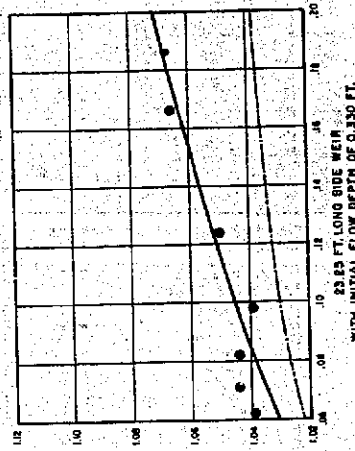
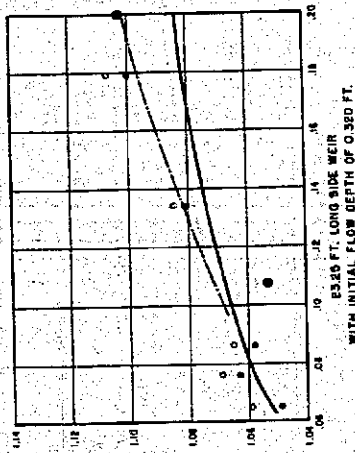
ATTENUATION OF SURGE WAVES BY A
SIDE WEIR IN A TRAPEZOIDAL CHANNEL
VARIATION OF AVERAGE SURGE VELOCITY
WITH FROUDE NUMBER OF INITIAL FLOW



●, ▲, ■ Experimental data from 8.00, 15.25
 and 23.25 ft. weir, respectively,
 for $F_0 = 0.186$.
 ○, △, □ Experimental data from 8.00, 15.25
 and 23.25 ft. weir, respectively,
 for $F_0 = 0.061$.
 F_0 = Froude number of initial flow
 where initial depth = the height
 of weir crest = 0.333 ft.

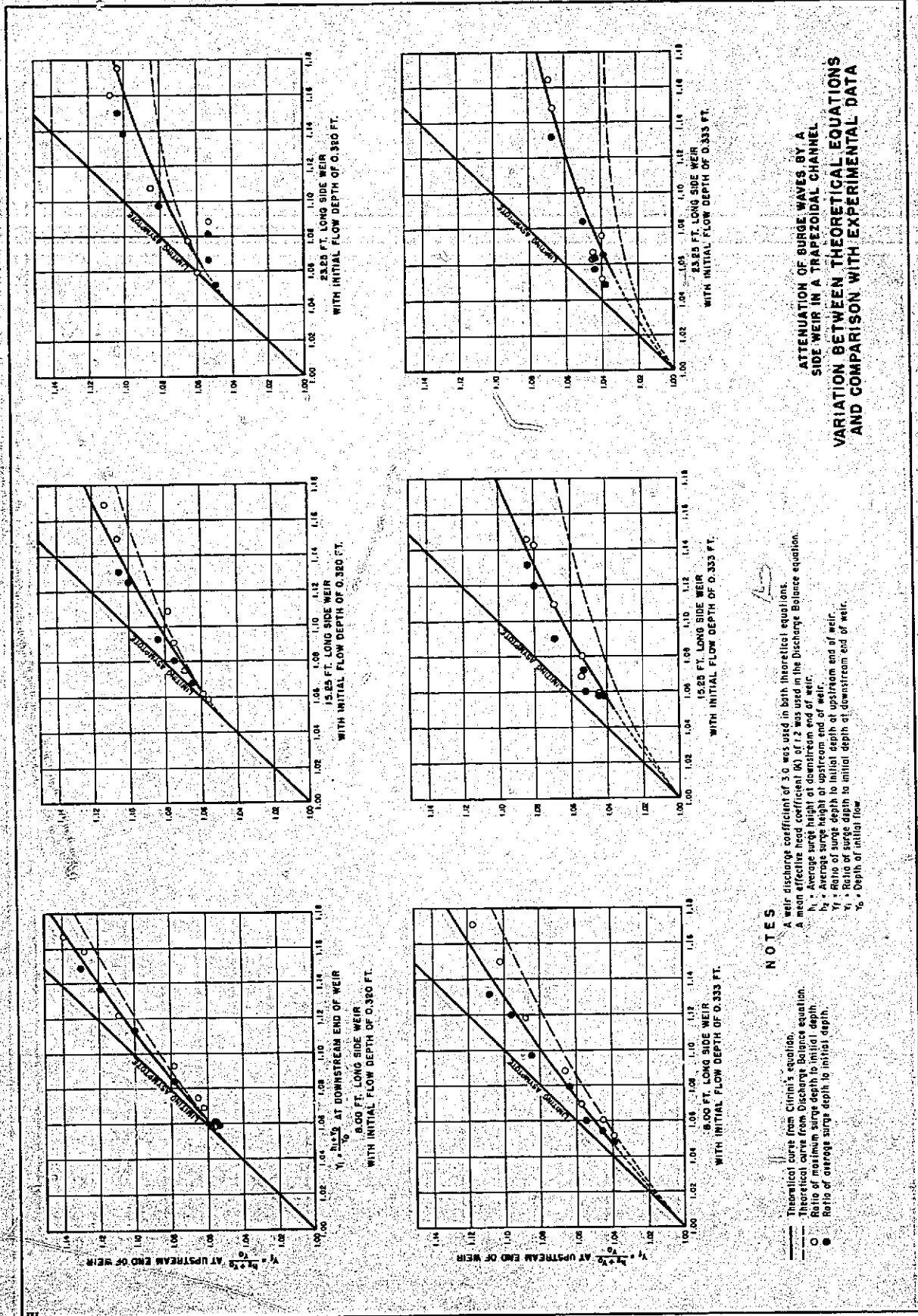
ATTENUATION OF SURGE WAVES BY A
 SIDE WEIR IN A TRAPEZOIDAL CHANNEL.
 EFFECT OF FROUDE NUMBER OF INITIAL
 FLOW ON ATTENUATING ABILITY OF WEIR

Figure 10
Report Hyd-575



ATTENUATION OF SURGE WAVES BY A
SIDE WEIR IN A TRAPEZOIDAL CHANNEL
EFFECT OF SIDE WEIR ON MAXIMUM
PEAKS AND AVERAGE SURGE HEIGHTS

NOTES
 A weir discharge coefficient of 3.0 was used in both theoretical equations.
 Discharge Balance Equation is equation (ii) in the text.
 h_0 = Ratio of maximum surge depth to initial flow depth.
 t_0 = Ratio of average surge depth to initial flow depth (2)
 T_0 = Fringe number of initial flow
 (1) Equation (2)

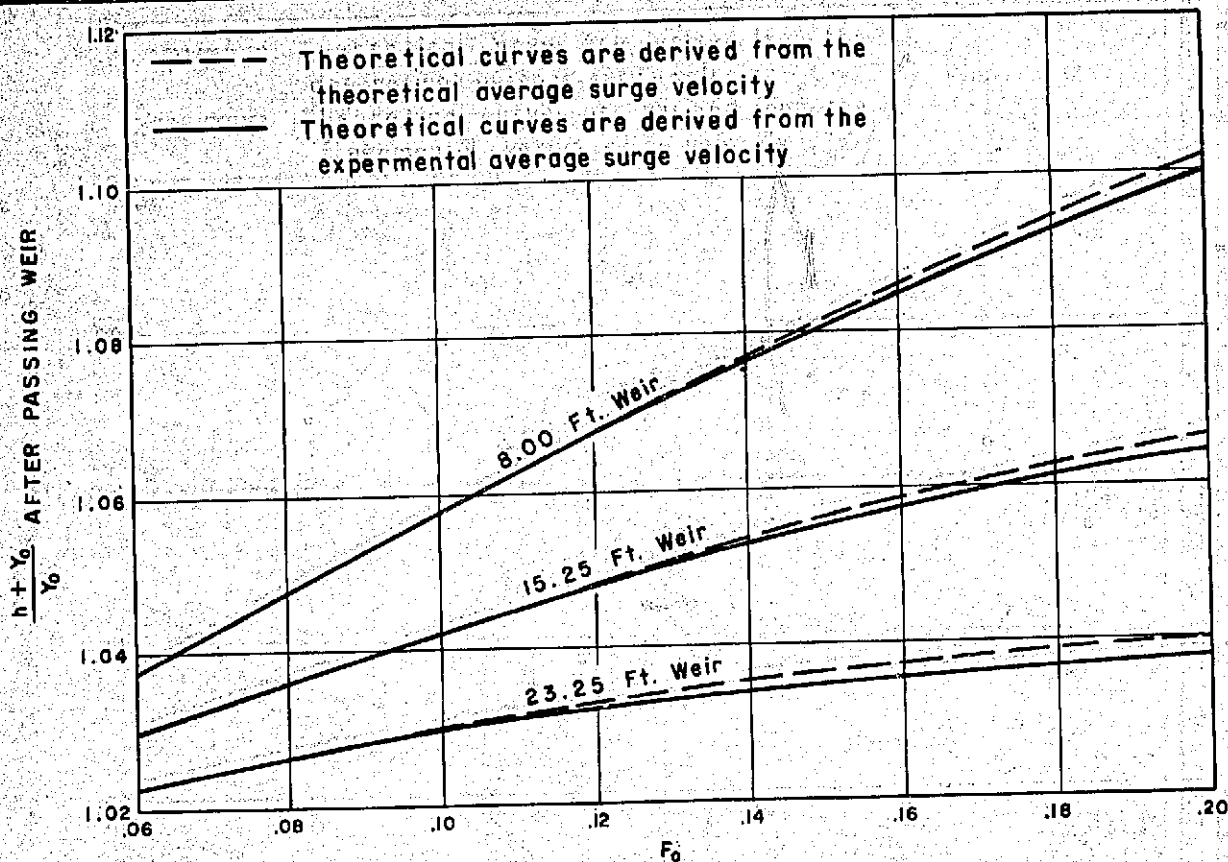


ATTENUATION OF SURGE WAVES BY A
SIDE WEIR IN A TRAPEZOIDAL CHANNEL
VARIATION BETWEEN THEORETICAL EQUATIONS
AND COMPARISON WITH EXPERIMENTAL DATA

NOTES

A weir discharge coefficient of 3.0 was used in both theoretical equations.
A mean effective head coefficient (K) of 1.2 was used in the Discharge Balance equation.
 h_1 = Average surge height at downstream end of weir.
 h_2 = Average surge height at upstream end of weir.
 y_1 = Ratio of surge depth to initial depth at upstream end of weir.
 y_2 = Ratio of surge depth to initial depth at downstream end of weir.
 y_0 = Depth of initial flow.

Theoretical curve from Ciriotti's equation.
Theoretical curve from Discharge Balance equation.
Ratio of maximum surge depth to initial depth.
Ratio of average surge depth to initial depth.



NOTES

Theoretical curves are derived from the discharge balance equation for a weir discharge coefficient of 3.0 and a mean effective head coefficient (K) of 1.2. See definitions on Figure 10.

ATTENUATION OF SURGE WAVES BY A SIDE WEIR IN A TRAPEZOIDAL CHANNEL
VARIATION OF THE DISCHARGE BALANCE EQUATION WITH DIFFERENT AVERAGE SURGE VELOCITIES

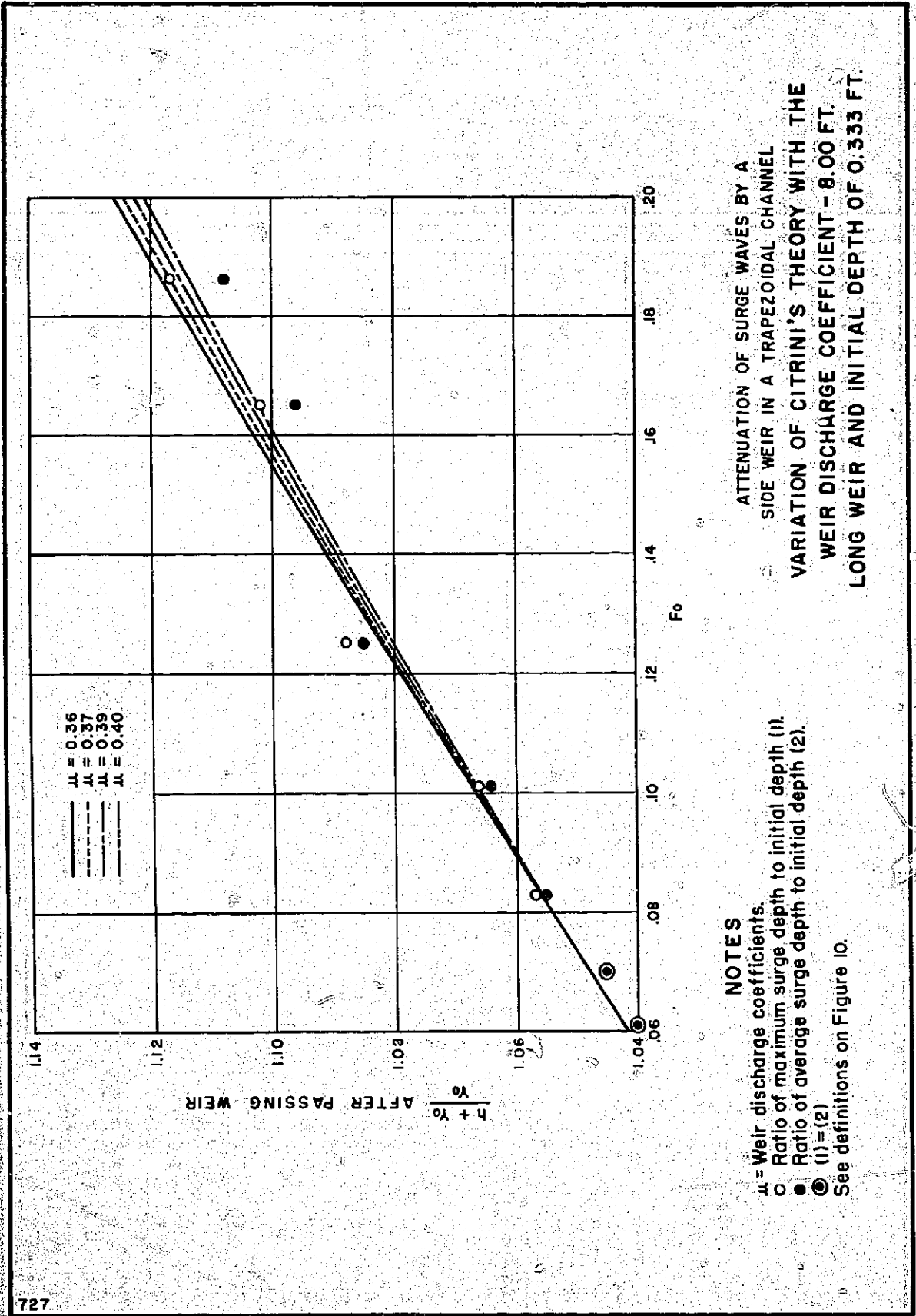
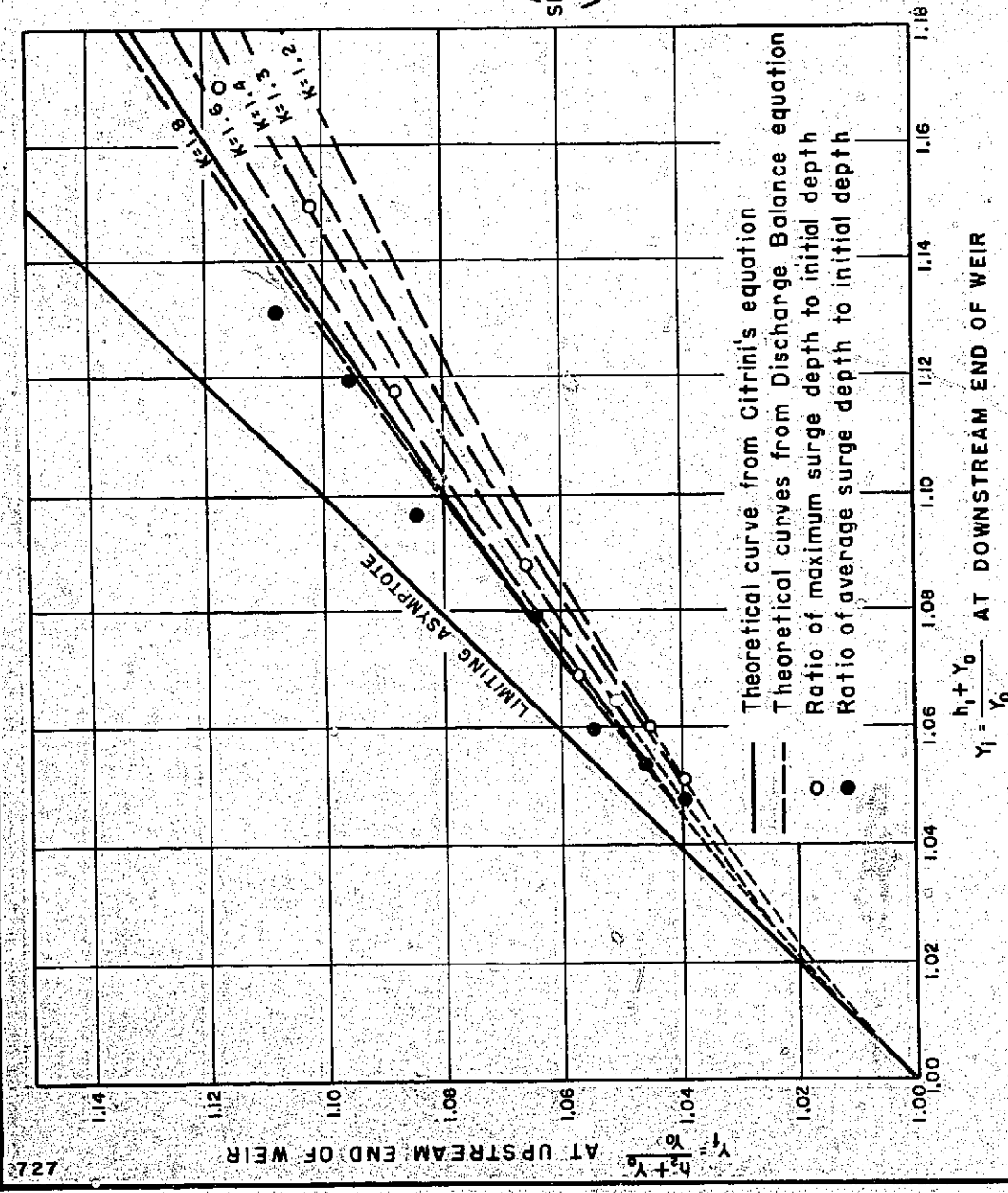


Figure 14
Report Hyd-575

NOTES

A weir discharge coefficient of 3.0 is used in both theoretical equations.
K-Coefficient of mean effective head on side weir.
Weir length 8.00 ft.
Initial depth 0.333 ft.
See definitions on Figure 11.

**ATTENUATION OF SURGE WAVES BY A SIDE WEIR IN A TRAPEZOIDAL CHANNEL
VARIATION OF THE DISCHARGE BALANCE EQUATION WITH DIFFERENT COEFFICIENTS OF MEAN EFFECTIVE HEAD ON THE SIDE WEIR**



APPENDIX

APPENDIX

PROGRAM NO. 1

Electronic Digital Computer Program to Solve the Theoretical Discharge Balance Equation for Attenuation of a Rejection Surge by a Side Weir in a Trapezoidal Channel

PROGRAM DESCRIPTION

The theoretical discharge balance equation, equation (1), and the weir discharge equation involve trial solution for the weir attenuated surge height (H_2). A computer program was developed for use on the Honeywell H-800 computing facility, U.S. Bureau of Reclamation, Denver, Colorado.

The program was written in the AUTOMATH (FORTRAN IV) program language. A listing of the program source statements and samples of the input and output data are included in this Appendix.

The average wave velocity (VW), and the average surge height at downstream end of the side weir (H_1) were obtained from the solutions of the theoretical equations which are shown in D. L. King's thesis [10]. Those equations also were solved by an electronic digital computer program which is described in the same paper [10].

Input data consist of the rejected rate of flow (QREJ), the average wave velocity (VW), the channel bottom width (B), the side slopes (S), the initial flow depth (Y1), the discharge coefficient of the side weir (COEF), the weir length (XL), the average surge height at the downstream end of the side weir (H_1), the coefficient of mean effective head on the side weir (RATIO), the distance of the weir crest above the channel floor (SPWYD), the Froude number of the initial flow (F), and the size (DELTA) of iteration steps used in the solution of the equations. The output data included all the input variables listed above, (except B, S, F and DELTA) the computed surge height (H_2) at the upstream end of the weir, the ratio of the surge depth to initial depth before (YI) and after (YF) attenuation by the weir, the reciprocal of the Froude number of the initial flow (RF), and an indicator of the accuracy of the approximate solution (FF).

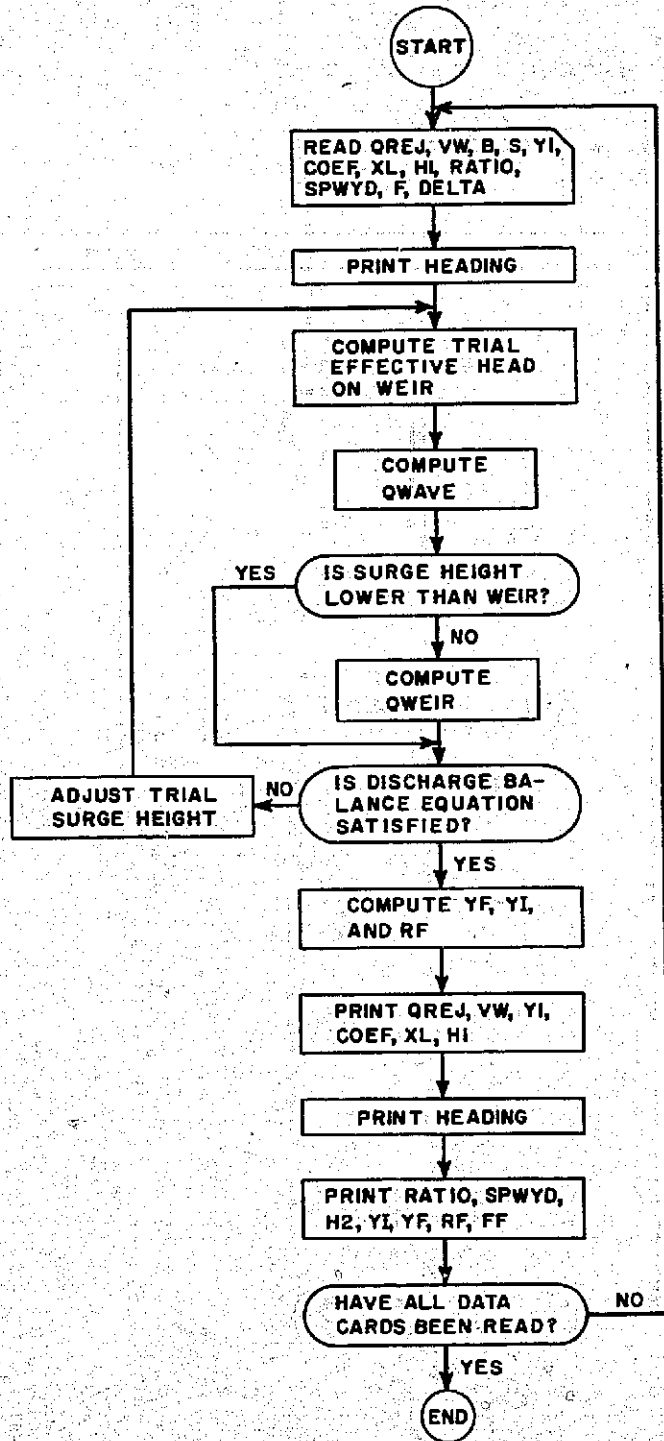
The bisection method is used to derive an approximate solution for the surge height following attenuation by a side weir. From the derived continuity equation and the weir discharge equation, the value of H_2 can be solved by trial and error. The algebraic sum $Q_{WAVE} + Q_{WEIR} - Q_{REJ}$, which is represented by FF in the program, is zero when the

correct value for H2 is obtained, or the correct solution is reached when the value of FF is within an arbitrarily chosen limit on either side of zero. In this case, the absolute value of FF required for a correct solution was assigned 0.00001. In the bisection method, the limits are adjusted and iterations continue until the solution is reached. For each iteration, the trial value of H2 is taken at the midpoint between the upper and lower limits. If the corresponding value of FF is found to be positive, the upper limit is assigned the trial value of H2 and the lower limit remains the same. If the value of FF is negative, the lower limit is assigned the trial value of H2 and the upper limit remains the same. Then a new trial H2 is obtained at the midpoint between the new limits. The procedure is repeated and the range between limits becomes smaller, until the correct solution is reached, or when the specified number of iterations has been performed. The final value of FF is printed as a check.

DEFINITION OF TERMS* USED IN COMPUTER PROGRAM NO. 1

DELTA	Size of iteration steps
FF	Indicator of accuracy of approximate solution
I	Loop counter
J	Loop counter
H1	h_1 in text
H2	h_2 in text
H2MIN	Minimum value of H_2
H2MAX	Maximum value of H_2
QREJ	Rejected discharge
QWAVE	Discharge of wave leaving upstream end of section
QWEIR	Discharge over side weir
RF	Reciprocal of Froude number of initial flow

*Terms which are identical to those defined in the main body of the report and some in computer program No. 2 are not repeated.



FLOW CHART FOR DIGITAL COMPUTER SOLUTION OF
THE DISCHARGE BALANCE EQUATION FOR SURGE
ATTENUATION BY A LATERAL SPILLWAY

```

C THEORETICAL ATTENUATION OF SURGE WAVES BY A SIDE WEIR
1 FORMAT (F8.0, 11F6.0)
2 FORMAT (1X,6F10.3)
30FORMAT (1H0,60H WHEN GREJ VW Y1 CCEF XL
1
40FORMAT (1H0,70H RATIO SPWYD Y1 YF
1
5 FORMAT (1X,6F10.3,F10.6)
6 READ (2,1) GREJ,VW,B,S,Y1,COEF,XL,H1,RATIO,SPWYD,F,DELTA
WRITE (3,3)
DO 9 I=1,100
H2MIN=0.0
H2MAX=H1+DELTA
DO 10 J=1,100
H2 = (H2MIN+H2MAX)/2.0
TRY=(H1+H2)/(2.0*RATIO) + Y1 - SPWYD
QWAVE = VW*(B + 2.0 *S*(Y1+H2/2.0))*H2
IF (TRY.LE. 0.0) GO TO 8
IF (TRY.GT.0.0) GO TO 81
8 FF = QWAVE - GREJ
GO TO 7
81 GWEIR = COEF*XL*TRY**1.5
FF = QWAVE + GWEIR - GREJ
7 IF (FF.LT.0.0) H2MIN=H2
IF (FF.GT.0.0) H2MAX=H2
IF (FF.EQ.0.0) GO TO 9
IF (ABS(FF).LE.0.00001) GO TO 9
10 CONTINUE
CALCULATION OF YF AND RF
9 YF = (H2+Y1)/Y1
Y1 = (H1+Y1)/Y1
RF = 1.0/F
WRITE (3,2) GREJ,VW,Y1,COEF,XL,H1
WRITE (3,4)
WRITE (3,5) RATIO,SPWYD,H2,Y1,YF,RF,FF
GO TO 6
END

```

IFN EFN

0001 1
 0002 2
 0003 3
 0004 4
 0005 5
 0006 7AC
 0007 7BC
 0010 7CC
 0011 8
 0012 9
 0013 10
 0014 10AR
 0015 10BR
 0016 11
 0017 11AA
 0020 12
 0021 13
 0022 14
 0023 14AA
 0024 22
 0025 23
 0026 14
 0027 16AD
 0030 16BD
 0031 16CD
 0032 16DD
 0033 25
 0034 29
 0035 30
 0036 30AA
 0037 31
 0040 32
 0041 33
 34
 35
 36

WHEN GREJ	.424	VW	2.779	Y1	.333	COEF	3.000	XL	8.000	H1	.056
RATIO	1.200	SPWYD	.333	H2	.033	YI	1.168	YF	1.100	RF	5.025
										FF	.000007
WHEN GREJ	.386	VW	2.794	Y1	.333	COEF	3.000	XL	8.000	H1	.050
RATIO	1.200	SPWYD	.333	H2	.031	YI	1.150	YF	1.094	RF	5.525
										FF	.000002
WHEN GREJ	.326	VW	2.818	Y1	.333	COEF	3.000	XL	8.000	H1	.042
RATIO	1.200	SPWYD	.333	H2	.027	YI	1.126	YF	1.082	RF	6.536
										FF	.000003
WHEN GREJ	.303	VW	2.827	Y1	.333	COEF	3.000	XL	8.000	H1	.039
RATIO	1.200	SPWYD	.333	H2	.026	YI	1.117	YF	1.077	RF	7.042
										FF	.000008
WHEN GREJ	.283	VW	2.835	Y1	.333	COEF	3.000	XL	8.000	H1	.037
RATIO	1.200	SPWYD	.333	H2	.024	YI	1.111	YF	1.073	RF	7.519
										FF	.000007

SAMPLE OUTPUT LISTING
PROGRAM No. 1

PROGRAM NO. 2

Electronic Digital Computer Program to Solve Citrini's Equation for Attenuation of a Rejection Surge by a Side Weir from (King [9])

PROGRAM DESCRIPTION

The program was developed to solve an equation derived by Citrini, [4] for the attenuation of an open channel surge by a side weir. The lengthy equation is presented in the Theoretical Considerations Section of this report and will not be repeated here. The program was written in the FORTRAN IV language and can be used on most electronic computers. No special operating procedures are required.

Solution of the equation was accomplished by the bisection method. The required result was the surge height following attenuation by the side weir (or lateral spillway). Dimensionless forms, YI and YF , were used in the computations. YI was the ratio of the surge depth ($Y2$) to the normal water depth ($Y1$) before attenuation by the weir, and YF was the corresponding ratio after attenuation by the weir. In the bisection method, upper and lower limits are chosen which are expected to bracket the correct solution. In this case, the upper limit ($YF1$) was the ratio of the surge depth before attenuation to the normal channel water depth (YI) and the lower limit ($YF2$) was assigned the value 1.0, which corresponds to complete destruction of the surge wave by the side weir. The trial value of YF is taken at the midpoint between the limits and substituted in the equation, which appears in the form of a function statement ($RESID$). The correct solution is reached when the value of the function is equal to zero or is within an arbitrarily chosen limit on either side of zero. In this case, the absolute value of the function required for a correct solution was 0.00001. In the bisection method, the limits are adjusted and iterations continue until the solution is obtained. For each iteration, the trial value of YF is taken at the midpoint between the upper and lower limits. If the corresponding value of $RESID$ is negative, the lower limit is assigned the trial value of YF and the upper limit remains the same. Then a new trial YF is obtained at the midpoint between the new limits. The procedure is repeated and the range between limits becomes smaller, until the correct solution is obtained or until 20 iterations (sufficient for the data used) had been accomplished. An error check was included, in case the method did not converge to the correct solution.

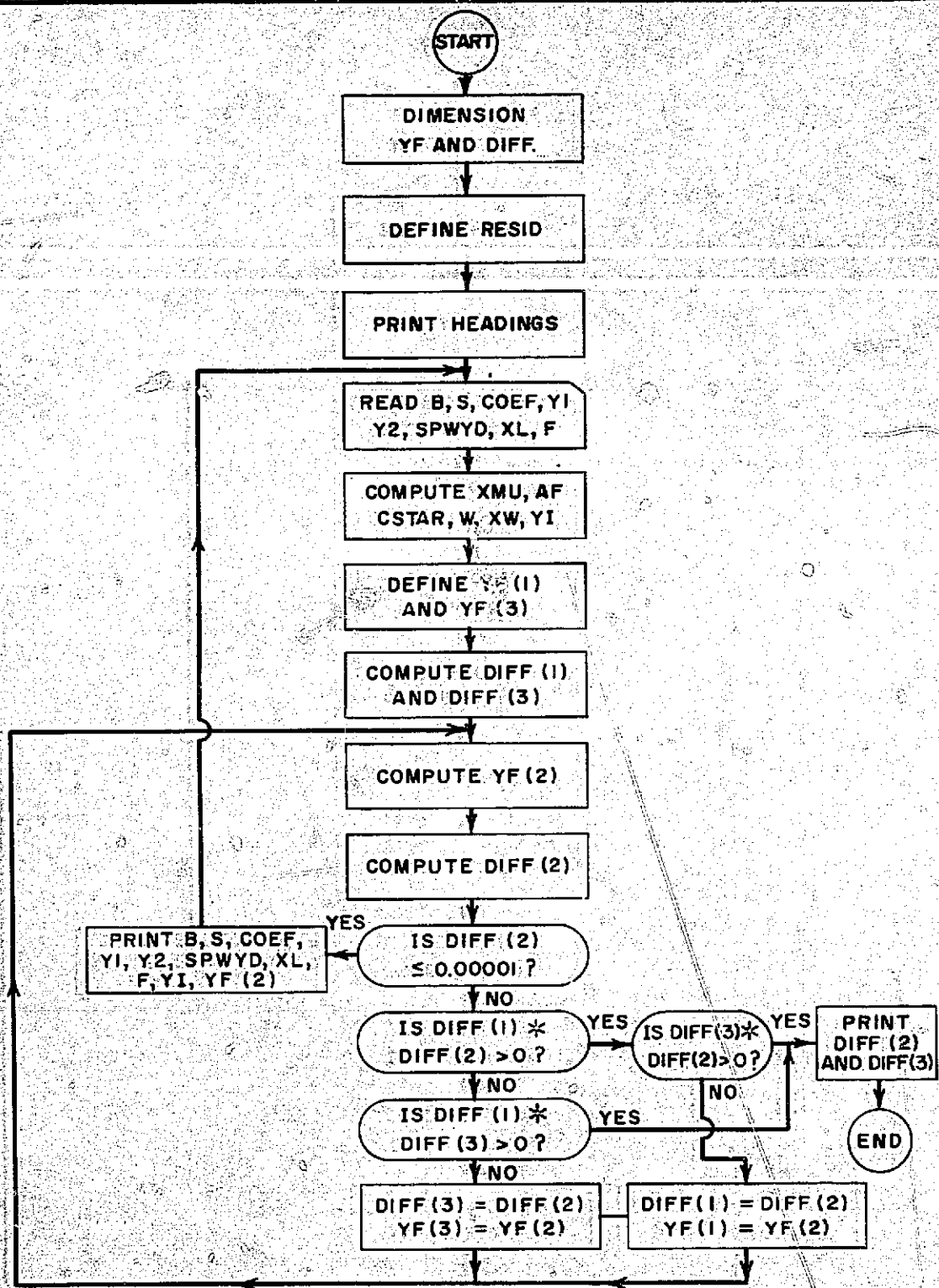
Input data consisted of the channel bottom width (B), the side slopes (S), the discharge coefficient of the side weir ($COEF$), the initial flow depth ($Y1$), the surge depth ($Y2$), the distance of the weir crest above the channel floor ($SPWYD$), the weir length (XL), and the Froude number of the initial flow (F). A sample input data sheet is included in this appendix.

The output data included the input variables listed above and the ratio of the surge depth to the initial depth before (YI) and after (YF) attenuation by the side weir. A representative output listing is also included in this appendix.

DEFINITION OF TERMS USED IN COMPUTER PROGRAM NO. 2

YF	Ratio of surge depth to initial depth following attenuation by the side weir (Y_f)
DIF	Value of equation for trial value of YF
RESID	Statement function name
YI	Ratio of surge depth to initial depth before attenuation by the side weir (Y_i)
XMU	Dimensionless weir discharge coefficient (μ)
XL	Weir length (L)
W	Width of channel at elevation of weir crest
AF	Reciprocal of Froude number of initial flow (A)
CSTAR	Ratio of SPWYD to YI (C*)
B	Channel bottom width
S	Channel side slopes
COEF	Weir discharge coefficient
Y1	Initial depth
Y2	Surge depth before attenuation by side weir
SPWYD	Height of weir crest above channel floor
F	Froude number of initial flow
XW	Ratio of weir length to channel top width at weir crest (L/W)
I	Subscript, fixed-point variable

*Terms in parenthesis are those which appear in original equation.



FLOW CHART FOR DIGITAL COMPUTER SOLUTION OF CITRINI'S EQUATION FOR SURGE ATTENUATION BY A LATERAL SPILLWAY

PROGRAM: HKATTN

JOE: 0831HKATTN

DETERMINATION OF SURGE ATTENUATION DUE TO CANAL SIDE SPILLWAY

```

0001 DIMENSION YF(3),C1FF(3)
0002 RESID(YF,YI,XMU,XL,M,AF,CSTAR) =
1 ((YF*(YI-1.0)*(1.0+0.75*(YI-1.0)))
2 + ((YI**2)-(YF**2))*((XL/M)*AF*(YF+YI)))
3 - ((XMU/2.0)*(XL/M)*AF*((YF+YI)**2)*((YF+YI)-2.*CSTAR)
4 - ((XMU/2.0)*(XL/M)*AF*((YF+YI)**2)*((YF+YI)-2.*CSTAR))
5 *((YF+YI)*AF*((YF**2)-1.0)*((YF+YI)-2.0*CSTAR))
6 *((YF+YI)*AF*((YF**2)-1.0)*((YF+YI)-2.0*CSTAR))
7 *AF*(YI-1.0)*((1.0+0.75*(YI-1.0)))
8 *AF*(YF+YI)*((YF+YI)**2)
13030FCR MAT(1H1,79H F YI YF)
1305 L
1305 FORMAT(1X,6F8.3,4F8.2,1X,3F8.3)
1330 FORMAT(8F8.0)
1330 WRITE(6,1303)
1331 READ(5,1330) B,S,COEF,Y1,Y2,SPWYD,XL,F
XMU = COEF/R,0199
AF = 1.0/F
CSTAR = SPWYD/Y1
B = B+2.0*S*SPWYD
XM = XL/M
Y1 = Y2/Y1
YF(1) = YI
YF(3) = 1.0
DO 1003 J=1,3,2
DIFF(J) = RESID(YF(1),YI,XMU,XL,M,AF,CSTAR)
1003 CONTINUE
DO 1005 J=1,20
YF(2) = (YF(1)+YF(3))/2.0
DIFF(2) = RESID(YF(2),YI,XMU,XL,M,AF,CSTAR)
IF(ABS(DIFF(2))) .LE. 0.00001) GO TO 1951
IF((DIFF(1)*DIFF(2)) .GT. 0.0) GO TO 1004
IF((DIFF(1)*DIFF(3)) .GT. 0.0) GO TO 1701
DIFF(3) = DIFF(2)
YF(3) = YF(2)
GO TO 1950
1004 IF((DIFF(3)*DIFF(2)) .GT. 0.0) GO TO 1701
DIFF(1) = DIFF(2)
YF(1) = YF(2)
1005 CONTINUE
1951 WRITE(6,1305) B,S,COEF,Y1,Y2,SPWYD,XL,F,YI,YF(2)
GO TO 1331
1700 FORMAT(9H,DIFF(1)=F,4)
1701 WRITE(6,1700) (DIFF(1),I=1,3)
END

```

LISTING OF PROGRAM SOURCE STATEMENTS PROGRAM No. 2

E	1.667	1.500	3.000	Y1	.333	SPWYD	8.00	F	.199	YI	1.168	YF	1.124
1.667	1.500	3.000	.333	.383	.333	5.00	.181	1.150	1.113	1.097	1.113	1.091	
1.667	1.500	3.000	.333	.375	.333	5.00	.153	1.126	1.091	1.087	1.091	1.076	
1.667	1.500	3.000	.333	.372	.333	5.00	.142	1.117	1.087	1.074	1.087	1.074	
1.667	1.500	3.000	.333	.370	.333	5.00	.133	1.111	1.078	1.063	1.096	1.070	
1.667	1.500	3.000	.333	.365	.333	5.00	.117	1.093	1.075	1.061	1.093	1.063	
1.667	1.500	3.000	.333	.364	.333	5.00	.111	1.087	1.072	1.059	1.087	1.061	
1.667	1.500	3.000	.333	.362	.333	5.00	.105	1.087	1.069	1.057	1.087	1.061	
1.667	1.500	3.000	.333	.359	.333	5.00	.095	1.078	1.066	1.054	1.078	1.061	
1.667	1.500	3.000	.333	.358	.333	5.00	.091	1.075	1.063	1.052	1.075	1.059	
1.667	1.500	3.000	.333	.357	.333	5.00	.086	1.072	1.060	1.048	1.072	1.057	
1.667	1.500	3.000	.333	.356	.333	5.00	.083	1.069	1.057	1.048	1.069	1.057	
1.667	1.500	3.000	.333	.355	.333	5.00	.080	1.066	1.054	1.045	1.066	1.054	
1.667	1.500	3.000	.333	.354	.333	5.00	.077	1.063	1.054	1.045	1.063	1.054	
1.667	1.500	3.000	.333	.353	.333	5.00	.074	1.060	1.054	1.045	1.060	1.054	
1.667	1.500	3.000	.333	.352	.333	5.00	.071	1.057	1.054	1.045	1.057	1.054	
1.667	1.500	3.000	.333	.352	.333	5.00	.069	1.057	1.054	1.045	1.057	1.054	
1.667	1.500	3.000	.333	.351	.333	5.00	.066	1.054	1.054	1.045	1.054	1.054	
1.667	1.500	3.000	.333	.351	.333	5.00	.064	1.054	1.054	1.045	1.054	1.054	
1.667	1.500	3.000	.333	.350	.333	5.00	.062	1.051	1.051	1.045	1.051	1.045	
1.667	1.500	3.000	.333	.349	.333	5.00	.059	1.048	1.048	1.045	1.048	1.045	

GPO 837-641

SAMPLE OUTPUT LISTING
PROGRAM No. 2

CONVERSION FACTORS--BRITISH TO METRIC UNITS OF MEASUREMENT

The following conversion factors adopted by the Bureau of Reclamation are those published by the American Society for Testing and Materials (ASTM Metric Practice Guide, January 1964) except that additional factors (*) commonly used in the Bureau have been added. Further discussion of definitions of quantities and units is given on pages 10-11 of the ASTM Metric Practice Guide.

The metric units and conversion factors adopted by the ASTM are based on the "International System of Units" (designated SI for Systeme International d'Unites), fixed by the International Committee for Weights and Measures; this system is also known as the Giorgi or MKSA (meter-kilogram (mass)-second-ampere) system. This system has been adopted by the International Organization for Standardization in ISO Recommendation R-31.

The metric technical unit of force is the kilogram-force; this is the force which, when applied to a body having a mass of 1 kg, gives it an acceleration of 9.80665 m/sec/sec, the standard acceleration of free fall toward the earth's center for sea level at 45 deg latitude. The metric unit of force in SI units is the newton (N), which is defined as that force which, when applied to a body having a mass of 1 kg, gives it an acceleration of 1 m/sec/sec. These units must be distinguished from the (inconstant) local weight of a body having a mass of 1 kg; that is, the weight of a body is that force with which a body is attracted to the earth and is equal to the mass of a body multiplied by the acceleration due to gravity. However, because it is general practice to use "pound" rather than the technically correct term "pound-force," the term "kilogram" (or derived mass unit) has been used in this guide instead of "kilogram-force" in expressing the conversion factors for forces. The newton unit of force will find increasing use, and is essential in SI units.

Table I

QUANTITIES AND UNITS OF SPACE

Multiply	By	To obtain
LENGTH		
Mill.	25.4 (exactly)	Micron
Inches	25.4 (exactly)	Millimeters
	2.54 (exactly)*	Centimeters
Feet	30.48 (exactly)	Centimeters
	0.3048 (exactly)*	Meters
	0.0003048 (exactly)*	Kilometers
Yards	0.9144 (exactly)	Meters
Miles (statute)	1,609.344 (exactly)*	Meters
	1.609344 (exactly)	Kilometers
AREA		
Square inches	6.4516 (exactly)	Square centimeters
Square feet	929.03*	Square centimeters
	0.092903	Square meters
Square yards	0.836127	Square meters
Acres	0.40469*	Hectares
	4,046.9*	Square meters
	0.0040469*	Square kilometers
Square miles	2.58999	Square kilometers
VOLUME		
Cubic inches	16.3871	Cubic centimeters
Cubic feet	0.0283168	Cubic meters
Cubic yards	0.764555	Cubic meters
CAPACITY		
Fluid ounces (U.S.)	29.5737	Cubic centimeters
	29.5729	Milliliters
Liquid pints (U.S.)	0.473179	Cubic decimeters
	0.473166	Liters
Quarts (U.S.)	946.358*	Cubic centimeters
	0.946331*	Liters
Gallons (U.S.)	3,785.43*	Cubic centimeters
	3.78543	Cubic decimeters
	3.78533	Liters
	0.00378543*	Cubic meters
Gallons (U.K.)	4.54609	Cubic decimeters
	4.54596	Liters
Cubic feet	28.3160	Liters
Cubic yards	764.55*	Liters
Acre-feet	1,233.5*	Cubic meters
	1,233,500*	Liters

Table II
QUANTITIES AND UNITS OF MECHANICS

Multiply	By	To obtain
WORK AND ENERGY*		
British thermal units (Btu)	0.262*	Kilogram calories
Btu per hour	1,055.06	Kg cal/hr m deg C
Foot-pounds	1.35582*	Joules per gram
		Joules
POWER		
Horsepower	746,000	Watts
Btu per hour	0.293071	Watts
Foot-pounds per second	1.35582	Watts
HEAT TRANSFER		
Btu in./hr ft ² deg F (k, thermal conductivity)	1.442	Milliwatts/cm deg C
Btu in./hr ft ² deg F (C, thermal resistance)	0.1740	Kg cal/hr m ² deg C
Btu/hr ft ² deg F (C, thermal conductance)	1.4850*	Milliwatts/cm ² deg C
Deg F hr ft ² /Btu (R, thermal resistance)	0.689	Kg cal/hr m ² deg C
Btu/lb deg F (c, heat capacity)	1.761	Deg C cm ³ /milliwatt
Btu/lb deg F (c, thermal diffusivity)	4.1868	1/deg C
ft ² /hr (thermal diffusivity)	1.7501	Cal/gram deg C
	0.2581	cm ² /sec
	0.09280*	M ² /hr
WATER VAPOR TRANSMISSION		
Grains/hr ft ² (water vapor transmission)	16.7	Grams/24 hr m ²
Perrns (permeance)	0.959	M ² /hr perm
Perm-inches (permeability)	1.87	Metric perm-centimeters

Table III
OTHER QUANTITIES AND UNITS

Multiply	By	To obtain
MASS		
Grains (1/7,000 lb)	64.79891 (exactly)	Milligrams
Troy ounces (480 grains)	31.1035	Grams
Avoirdupois ounces (437.5 grains)	28.3496	Grams
Pounds (avoirdupois)	0.45359237 (exactly)	Kilograms
Short tons (2,000 lb)	907.185	kilograms
Long tons (2,240 lb)	1,016.05	kilograms
FORCE/AREA		
Pounds per square inch	0.070307	Kilograms per square centimeter
Pounds per square foot	0.889476	Newtons per square centimeter
	4.88243	Kilograms per square meter
	47.8803	Newtons per square meter
MASS/VOLUME DENSITY		
Ounces per cubic inch	1.72889	Grams per cubic centimeter
Pounds per cubic foot	16.0185	Kilograms per cubic meter
Tons (long) per cubic yard	0.160106	Grams per cubic centimeter
	1.32894	Grams per cubic centimeter
MASS/CAPACITY		
Ounces per gallon (U. S.)	7.4883	Grams per liter
Ounces per gallon (U. K.)	0.2302	Grams per liter
Pounds per gallon (U. S.)	119.829	Grams per liter
Pounds per gallon (U. K.)	99.779	Grams per liter
BENDING MOMENT OR TORQUE		
Inch-pounds	0.01821	Meter-kilograms
Foot-pounds	1.2548 x 10 ⁶	Centimeter-dynes
	0.35526 x 10 ⁷	Meter-kilograms
Foot-pounds per inch	5.4431	Centimeter-dynes
Ounces-inches	72.033	Gram-centimeters
VELOCITY		
Feet per second	30.48 (exactly)	Centimeters per second
Feet per year	0.3048 (exactly)*	Meters per second
Miles per hour	0.88496 x 10 ⁻⁶	Centimeters per second
	1.609344 (exactly)	Meters per second
	0.44704 (exactly)	Meters per second
ACCELERATION*		
Feet per second ²	0.3048*	Meters per second ²
FLOW		
Cubic feet per second (second-foot)	0.028317*	Cubic meters per second
Cubic feet per minute	0.4719	Liters per second
Gallons (U. S.) per minute	0.06308	Liters per second
FORCE*		
Pounds	0.453592*	Kilograms
	4.4482*	Newtons
	4.4482 x 10 ⁻⁵ *	Dynes

ABSTRACT

Theoretical equations and supporting experimental data are presented for determining attenuation of surge waves by a longitudinal side weir in a trapezoidal channel. Comparisons are made of a theoretical equation which had been derived previously for rectangular channels and an equation developed during this study; agreement of each of these equations with experimental data is determined. Surge heights were recorded by 6 capacitance-type wave probes with sensors consisting of plasticized-enamel-coated wire. Two short digital computer programs were developed for trial solutions of the theoretical equations. An explanation of each program, source statement listing, sample input data, and results are presented in the appendix.

ABSTRACT

Theoretical equations and supporting experimental data are presented for determining attenuation of surge waves by a longitudinal side weir in a trapezoidal channel. Comparisons are made of a theoretical equation which had been derived previously for rectangular channels and an equation developed during this study; agreement of each of these equations with experimental data is determined. Surge heights were recorded by 6 capacitance-type wave probes with sensors consisting of plasticized-enamel-coated wire. Two short digital computer programs were developed for trial solutions of the theoretical equations. An explanation of each program, source statement listing, sample input data, and results are presented in the appendix.

ABSTRACT

Theoretical equations and supporting experimental data are presented for determining attenuation of surge waves by a longitudinal side weir in a trapezoidal channel. Comparisons are made of a theoretical equation which had been derived previously for rectangular channels and an equation developed during this study; agreement of each of these equations with experimental data is determined. Surge heights were recorded by 6 capacitance-type wave probes with sensors consisting of plasticized-enamel-coated wire. Two short digital computer programs were developed for trial solutions of the theoretical equations. An explanation of each program, source statement listing, sample input data, and results are presented in the appendix.

ABSTRACT

Theoretical equations and supporting experimental data are presented for determining attenuation of surge waves by a longitudinal side weir in a trapezoidal channel. Comparisons are made of a theoretical equation which had been derived previously for rectangular channels and an equation developed during this study; agreement of each of these equations with experimental data is determined. Surge heights were recorded by 6 capacitance-type wave probes with sensors consisting of plasticized-enamel-coated wire. Two short digital computer programs were developed for trial solutions of the theoretical equations. An explanation of each program, source statement listing, sample input data, and results are presented in the appendix.

Ryd-575

Rungroongtaanin, S and King, D L
ATTENUATION OF SURGE WAVES BY A SLIDE WEIR IN A TRAPEZOIDAL CHANNEL
USBR Lab Rept Ryd-575, Ryd Br, Apr 1967. Bureau of Reclamation, Denver,
47 p, 14 fig, 4 tab, 13 ref

DESCRIPTORS-- canals/ model tests/ *surges/ *trapezoidal channels/ weirs/
hydraulic transients// bore /wave// Froude number/ transitory waves/
unsteady flow/ calibrations/ instrumentation/ measuring instruments/
recording systems/ capacitance/ dielectrics/ electronic equipment/ research
and development/ oscillographs/ computer programming/ mathematical
analysis/ hydraulic models
IDENTIFIERS-- wave probes/ Citrini equation

Ryd-575

Rungroongtaanin, S and King, D L
ATTENUATION OF SURGE WAVES BY A SLIDE WEIR IN A TRAPEZOIDAL CHANNEL
USBR Lab Rept Ryd-575, Ryd Br, Apr 1967. Bureau of Reclamation, Denver,
47 p, 14 fig, 4 tab, 13 ref

DESCRIPTORS-- canals/ model tests/ *surges/ *trapezoidal channels/ weirs/
hydraulic transients// bore /wave// Froude number/ transitory waves/
unsteady flow/ calibrations/ instrumentation/ measuring instruments/
recording systems/ capacitance/ dielectrics/ electronic equipment/ research
and development/ oscillographs/ computer programming/ mathematical
analysis/ hydraulic models
IDENTIFIERS-- wave probes/ Citrini equation

Ryd-575

Rungroongtaanin, S and King, D L
ATTENUATION OF SURGE WAVES BY A SLIDE WEIR IN A TRAPEZOIDAL CHANNEL
USBR Lab Rept Ryd-575, Ryd Br, Apr 1967. Bureau of Reclamation, Denver,
47 p, 14 fig, 4 tab, 13 ref

DESCRIPTORS-- canals/ model tests/ *surges/ *trapezoidal channels/ weirs/
hydraulic transients// bore /wave// Froude number/ transitory waves/
unsteady flow/ calibrations/ instrumentation/ measuring instruments/
recording systems/ capacitance/ dielectrics/ electronic equipment/ research
and development/ oscillographs/ computer programming/ mathematical
analysis/ hydraulic models
IDENTIFIERS-- wave probes/ Citrini equation

Ryd-575

Rungroongtaanin, S and King, D L
ATTENUATION OF SURGE WAVES BY A SLIDE WEIR IN A TRAPEZOIDAL CHANNEL
USBR Lab Rept Ryd-575, Ryd Br, Apr 1967. Bureau of Reclamation, Denver,
47 p, 14 fig, 4 tab, 13 ref

DESCRIPTORS-- canals/ model tests/ *surges/ *trapezoidal channels/ weirs/
hydraulic transients// bore /wave// Froude number/ transitory waves/
unsteady flow/ calibrations/ instrumentation/ measuring instruments/
recording systems/ capacitance/ dielectrics/ electronic equipment/ research
and development/ oscillographs/ computer programming/ mathematical
analysis/ hydraulic models
IDENTIFIERS-- wave probes/ Citrini equation